Cell Cycle 13:18, 2913–2930; September 15, 2014; © 2014 Taylor & Francis Group, LLC

A knockdown with smoke model reveals FHIT as a repressor of Heme oxygenase 1

Jennifer A Boylston and Charles Brenner*

Department of Biochemistry and Program in Molecular and Cellular Biology; Carver College of Medicine; University of Iowa; Iowa City, IA USA

Keywords: BACH1, Cigarette smoke, FHIT, HMOX1, NRF2, Oxidative Stress

Abbreviations: ApppA, diadenosine triphosphate; ARE, antioxidant response element; *BACH1*, BTB and CNC homology 1 gene; BMC, bone marrow cell; *CPT*, camptothecin; *CSE*, cigarette smoke extract; *FHIT*, fragile histidine triad gene; *HMOX1*, heme oxygenase 1 gene; MMC, mitomycin C; Nrf2, nuclear factor erythroid derived 2-like 2 protein; qRT-PCR, quantitative real time PCR; RNAi, RNA interference; ROS, reactive oxygen species; siRNA, short interfering RNA.

Fragile histidine triad (*FHIT*) gene deletions are among the earliest and most frequent events in carcinogenesis, particularly in carcinogen-exposed tissues. Though *FHIT* has been established as an authentic tumor suppressor, the mechanism underlying tumor suppression remains opaque. Most experiments designed to clarify *FHIT* function have analyzed the consequence of re-expressing *FHIT* in *FHIT*-negative cells. However, carcinogenesis occurs in cells that transition from *FHIT*-positive to *FHIT*-negative. To better understand cancer development, we induced *FHIT* loss in human bronchial epithelial cells with RNA interference. Because *FHIT* is a demonstrated target of carcinogens in cigarette smoke, we combined *FHIT* silencing with cigarette smoke extract (CSE) exposure and measured gene expression consequences by RNA microarray. The data indicate that *FHIT* loss enhances the expression of a set of oxidative stress response genes after exposure to CSE, including the cytoprotective enzyme heme oxygenase 1 (*HMOX1*) at the RNA and protein levels. Data are consistent with a mechanism in which Fhit protein is required for accumulation of the transcriptional repressor of *HMOX1*, Bach1 protein. We posit that by allowing superinduction of oxidative stress response genes, loss of *FHIT* creates a survival advantage that promotes carcinogenesis.

Introduction

The fragile histidine triad gene (*FHIT*) is a tumor suppressor that spans the most common fragile site in the human genome, *FRA3B*.[1-3] *FHIT* is constitutively expressed in most tissues, and its loss is associated with a diverse set of malignancies, including lung, stomach, colon, breast and skin carcinomas.[1,4-11] Tumors expressing loss of *FHIT* are typically of epithelial origin, and *FHIT* has been shown to be a common target of carcinogens, particularly cigarette smoke.[12-15] Exposure to cigarette smoke is associated with *FHIT* exon deletion and translocation, as well as hypermethylation of the *FHIT* promoter with consequent loss of Fhit protein and development of malignancy.[5,9,16,17]

Previous work clearly demonstrates the tumor suppressor activity of *FHIT*. Mice heterozygous at the locus are more susceptible to spontaneous tumor formation.[1,18] Tumor formation is accelerated by treatment with chemical carcinogens and can be prevented with *FHIT* gene therapy.[1,3,19] Cell culture models show that re-expression of *FHIT* in *FHIT*-negative cells induces apoptosis, but the precise molecular mechanisms underlying tumor suppression remain unclear.[4,6,20] Recent experiments demonstrate that Fhit deficiency promotes epithelial-mesenchymal transition, that *FHIT* expression protects genome integrity after carcinogen treatment, and also establish a role for Fhit in mitochondrial biology.[21-27]

Hanahan and Weinberg summarized that cancer cells are marked by the gain of 6 abnormal behaviors.[12,14,28] Genome instability and subsequent genetic alterations underlie the acquisition of the hallmarks of cancer, as successive alterations in DNA produce genotypes that confer selective advantages. Frequent loss of *FHIT* in tumors is well documented.[5,9,16,29] Of equal significance, *FHIT* inactivation occurs early in the process of carcinogenesis, particularly in lung cancer,[18,30] suggesting that loss of this gene may facilitate acquisition of the additional alterations required for cell transformation.

Carcinogenesis occurs when cells lose expression of tumor suppressor genes. However, most experiments designed to dissect the mechanism of the *FHIT* gene were performed by converting $FHIT^{-}$ cells to $FHIT^{+}$. Here we used RNA interference (RNAi) to model early *FHIT* loss in bronchial epithelial cells. When *FHIT* deficient cells were exposed to cigarette smoke, we saw that expression of a set of genes involved in the oxidative stress response was enhanced, including the cytoprotective enzyme heme oxygenase 1 (*HMOX1*).

HMOX1 expression is induced in response to various insults such as exposure to heavy metals, ultraviolet light, inflammation,

*Correspondence to: Charles Brenner; Email: charles-brenner@uiowa.edu
Submitted: 05/21/2014; Revised: 06/21/2014; Accepted: 06/23/2014
http://dx.doi.org/10.4161/15384101.2014.946858

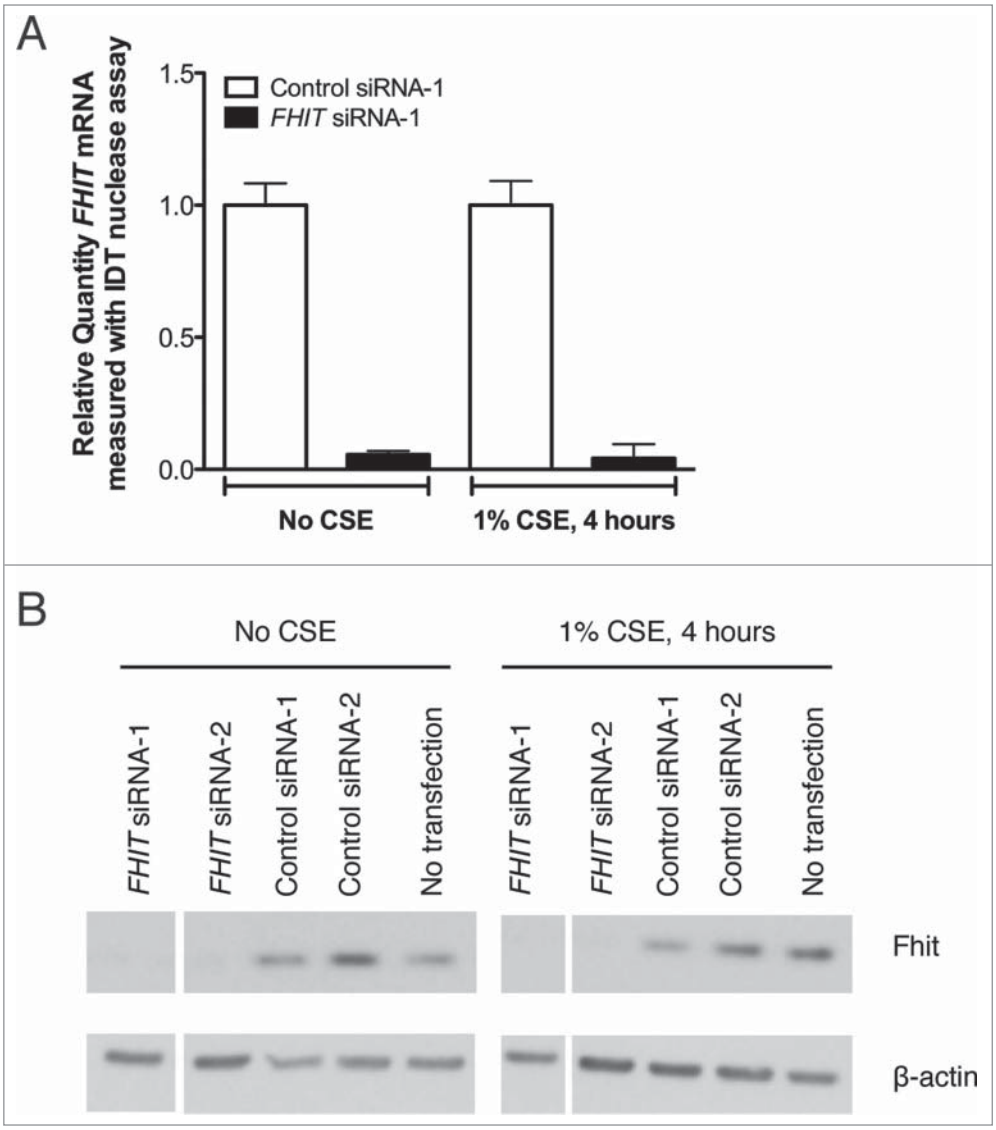

Figure 1. *FHIT* siRNA significantly reduces expression of *FHIT* mRNA and protein. HBEC3-TK cells were transfected with control or *FHIT*-targeting siRNAs for 48 hours. Cells were then exposed to 1% CSE for 4 hours or were left untreated. (**A**) Decreased *FHIT* expression was determined by qRT-PCR. Data represent the results of five experiments. (**B**) Fhit protein abundance was assessed by western blot. Treatment with 2 *FHIT*-targeting siRNAs significantly reduces Fhit protein levels and treatment with 2 negative control siRNAs does not affect Fhit protein levels. β-actin serves as an internal standard for loading control. Data represent the results of five experiments.

and oxidative stress.[19,31] *HMOX1* expression protects cells from dying during acute exposure to stresses, but the mechanisms underlying this function are not fully understood. It has been proposed that the byproducts of Hmox1-catalyzed breakdown of heme, carbon monoxide and bilirubin, underlie cytoprotection by maintaining reactive oxygen species (ROS) homeostasis and promoting a cellular anti-oxidant state.[20,32] However, expression of a catalytically inactive Hmox1 mutant promotes cell survival after stress as well as the wild type protein, suggesting that Hmox1 cytoprotection functions through an independent, yet to be elucidated mechanism.[28,33] Early events that occur after Hmox1 expression include increased cell proliferative capacity,[29,34] decreased cell adhesion,[30,35] increased migration potential,[31,35,36] and evasion of apoptosis.[32,37] It follows that *HMOX1* overexpression is detected in many cancers, including prostate malignancies, melanoma, glioma, adenocarcinoma, and others.[17,33,38]

Here, we demonstrate that loss of Fhit in bronchial epithelial cells promotes enhanced and sustained induction of Hmox1 in response to cigarette smoke exposure. We investigated the mechanism by which Fhit modulates Hmox1 expression and determined that Fhit loss is associated with decreased expression of a primary transcriptional repressor of *HMOX1*, Bach1. Thus, Fhit may be required for the normal cellular response to oxidative stress.

Table 1. Gene expression changes in *siFHIT* versus *siControl* treated HBEC3-TK cells

Gene_assignment	Gene Symbol	p-value	Ratio	Fold Change siFHIT over siControl
NM_021155 // CD209 // CD209 molecule // 19p13 // 30835 /// NR_026692 // CD209 // CD209	CD209	0.0338	2.04	2.04
AK126520 // BIVM // basic, immunoglobulin-like variable motif containing // 13q33.1 //	BIVM	0.0158	2.57	2.57
ENST00000391728 // KIR3DL1 // killer cell immunoglobulin-like receptor, three domains,	KIR3DL1	0.0340	3.04	3.04

We propose that by inactivating a system that attenuates antioxidant responses, loss of *FHIT* provides epithelial cells a survival advantage that promotes carcinogenesis.

Results

Gene expression changes in response to *FHIT* knockdown

The mechanism by which *FHIT* functions as a tumor suppressor has not been fully explained by experiments in which the *FHIT* gene has been reintroduced to *FHIT* negative cells. To investigate the hypothesis that Fhit acts as a regulator of gene expression in bronchial epithelial cells, we performed microarray analysis of cells after knocking down *FHIT* expression with siRNA. HBEC3-TK is an immortalized bronchial epithelial cell line that has been used to study the consequences of gene inactivation in lung cancer.[13,35] These cells display normal epithelial morphology, are not transformed, have an intact p53 pathway, and have been used by others to study the pathogenesis of lung cancer.[35,36,39] We first determined that treatment of HBEC3-TK cells with 2 unique siRNAs robustly silences *FHIT* expression at both the mRNA and protein level (**Fig. 1 A, B**). Total RNA from treated cells was analyzed by microarray to assess transcriptome changes due to *FHIT* loss. After restricting the data set to expression changes $\geq$1.5-fold with $P \leq 0.05$ followed by multiple testing correction with a false discovery rate, we observed changes in only 3 genes, suggesting that *FHIT* loss does not have a large impact on gene expression in this model (**Table 1**).

The *FHIT* gene, which encompasses the common fragile site at 3p14.2, is a known target

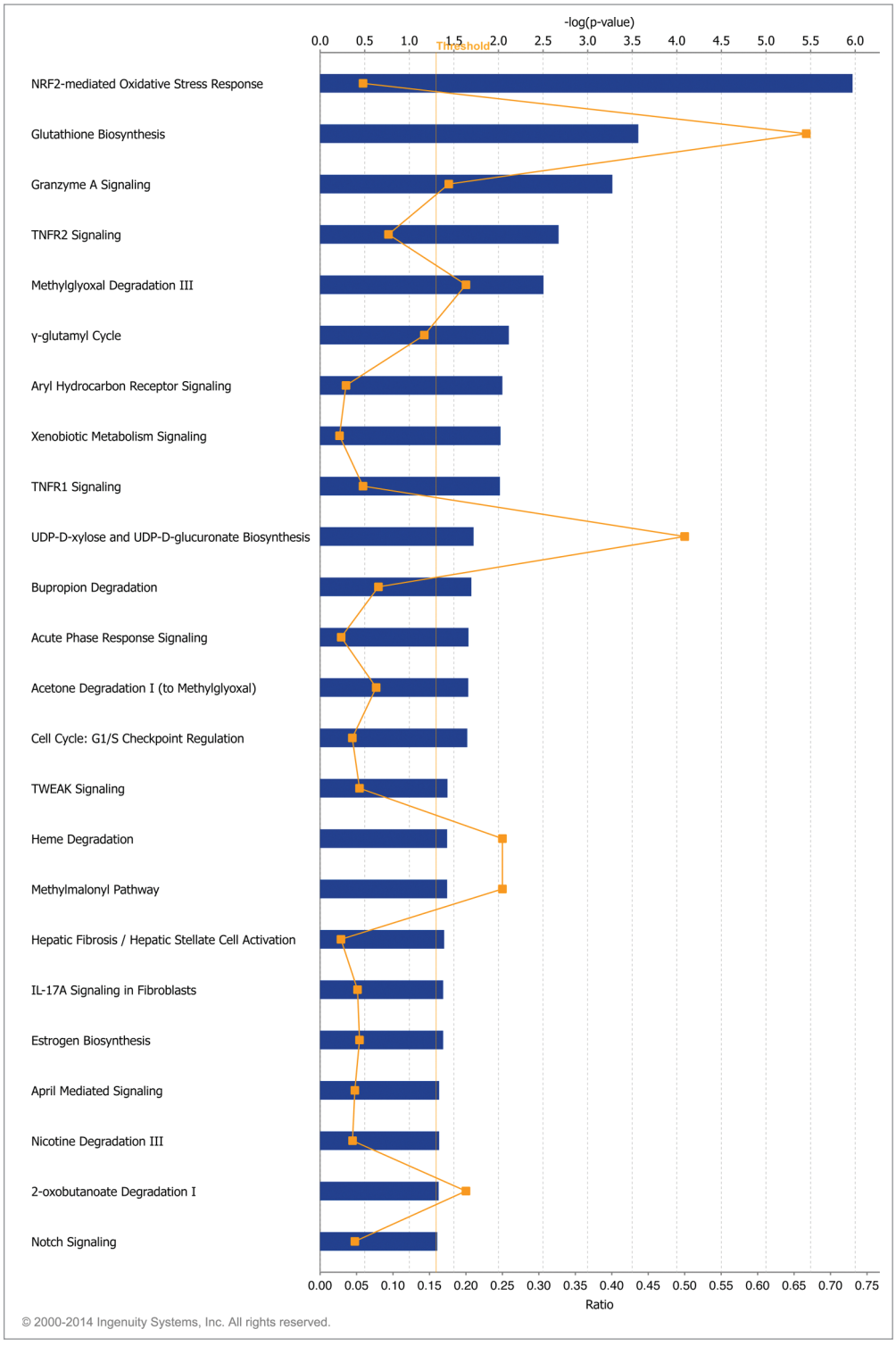

Figure 2. Canonical pathways affected by cigarette smoke exposure. Gene expression changes between cells treated with *siControl* (48 h) plus 1% CSE (4 h) and cells treated with *siControl* (48 h) alone were determined by microarray. IPA core analysis was used to generate a list of top biological functions affected by CSE exposure. The significant canonical pathways affected by CSE exposure are represented. x-axis bars represent the [–log(p-value)] of the pathway, calculated by Fisher's exact test. The threshold for this analysis was set to *P*-value$\leq$0.05. x-axis points (orange) represent the ratio calculated by dividing the number of differentially expressed genes that map to a particular pathway by the total number of genes in that pathway.

Table 2. Gene expression changes in response to treatment with 1% CSE in *siControl* treated HBEC3-TK cells

Gene assignment	Gene symbol	Gene description	p-value	Fold change: *siControl* plus CSE over *siControl* no CSE
NM_002133	HMOX1	Heme oxygenase decycling 1	8.67E-05	13.63
NM_02099	AKR1B10	Aldo-ketoreductase family 1, member B10	6.31E-05	6.41
NM_014331	SLC7A11	Solute carrier family 7	1.61E-04	6.16
NM_002061	GCLM	Glutamate-cysteine ligase, modifier subunit	7.87E-06	4.19
NM_032145	FBX030	F-box protein 30	1.28E-06	3.03
NM_001354	AKR1C2	Aldo-ketoreductase family 1, member C2	1.32E-04	2.94
NM_000146	FTL	Ferritin, light polypeptide	1.13E-04	2.86
NM_007034	DNAJB4	DnaJ (Hsp40) homolog, subfamily B, member 4	3.31E-05	2.79
NM_032717	AGPAT9	Acylglycerol-3-phosphate O-acyltransferase 9	1.19E-07	2.61
NM_080725	SRXN1	Sulfiredoxin 1	8.73E-06	2.48
NM_00330	TXNRD1	Thioredoxin reductase 1	2.15E-06	2.48
NM_006912	RIT1	Ras-like without CAAX 1	5.69E-06	2.38
NM_001498	GCLC	Glutamate-cysteine ligase, catalytic subunit	5.12E-05	2.33
NM_003714	STC2	Stanniocalcin 2	9.40E-05	2.29
NM_003359	UGHD	UDP-glucose 6-dehydrogenase	4.24E-06	2.22
NM_012124	CHORDC1	Cysteine and histidine-rice domain (CHORD)-containing 1	9.51E-06	1.99
NM_001037330	TRIM16L	Tripartite motif-containing 16-like	1.45E-06	1.93
NM_022060	ABHD4	Abhydrolase domain containing 4	7.20E-05	1.82
NM_001432	EREG	Epiregulin	1.64E-04	1.77
NM_018169	C12orf35	Chromosome 12 open reading frame 35	8.07E-05	1.65
NM_002032	FTH1	Ferritin, heavy polypeptide 1	4.26E-06	1.62
NM_000903	NQO1	NADPH dehydrogenase, quinone 1	1.09E-05	1.56
NM_005186	CAPN1	Calpain 1, large subunit	3.64E-05	−1.54
NR_027244	LOC151009	Hypothetical LOC151009	5.22E-05	−1.57
NM_014640	TTLL4	Tubulin tyrosine ligase-like family, member 4	6.87E-05	−1.58
NM_152683	CCDC111	Coiled-coil domain containing 111	5.51E-07	−1.59
NM_003545	HIST1H4E	Histone cluster 1, H4e	1.44E-04	−1.64
NM_183047	ZMYND8	Zinc finger, MYND-type containing 8	1.13E-04	−1.66
NM_020529	NFKBIA	Nuclear factor of kappa light polypeptide gene enhancer in B-cell	2.24E-06	−1.80
NR_002433	SNORD12C	Small nucleolar RNA, C/D box 12C	1.13E-04	−1.80
NM_002192	INHBA	Inhibin, β A	1.14E-04	−2.50
NM_006977	ZBTB25	Zinc finger and BTB domain containing 25	1.10E-04	−2.56

of environmental carcinogens including cigarette smoke. Loss of heterozygosity at 3p14 occurs more commonly in smokers than in nonsmokers.[37,40] Preneoplastic lesions of the lung and cervix show a greater frequency of *FHIT* loss in smokers than in nonsmokers.[17,38,41] Rats exposed to cigarette smoke for short time intervals show a time dependent decrease in *FHIT* expression at both mRNA and protein levels in bronchial epithelial cells.[15,42]. Furthermore, peripheral blood samples show that active smokers express fragility at the *FHIT* locus.[13,43-45] Relying on these data, we hypothesized that *FHIT* plays a role in mediating the cellular response to cigarette smoke. To test this, siRNA-treated HBEC3-TK cells were exposed to 1% CSE for 4 hours prior to RNA extraction and microarray analysis. We first aimed to establish that our CSE treatment protocol impacted gene expression in an expected manner. To do this, we compared gene expression in cells treated with *siControl* plus 1% CSE to gene expression in cells treated with *siControl* only. After restricting the dataset to expression changes $\geqq$1.5-fold with $P \leqq 0.05$ followed by multiple testing correction with a false discovery rate, we observed changes in 378 genes, indicating that the CSE treatment had a strong effect on gene expression. These differentially expressed genes were analyzed with Ingenuity Pathway Analysis (IPA, Ingenuity Systems, www.ingenuity.com) to determine what molecular pathways were altered by CSE treatment. The significant canonical pathways associated with the differentially expressed genes are presented (**Fig. 2**). The affected pathways included NRF2-mediated oxidative stress response, glutathione biosynthesis, aryl hydrocarbon receptor signaling, and xenobiotic metabolism signaling, among others. This result is consistent with previous reports that these pathways are affected by exposing cells in culture to cigarette smoke.[46-50] To assess the combined effect of *FHIT* knockdown and CSE treatment, we applied the same analysis criteria used for cells that were not treated with CSE to analyze the gene expression consequences of CSE treatment in control and *FHIT* knockdown cells (**Tables 2**, **3**). We determined that a set of genes involved in the cytoprotective oxidative stress response were either only activated in *FHIT* knockdown cells, or were activated in both *FHIT* knockdown and control cells, but gene expression was enhanced by *FHIT* loss. Notably, a subset of the dysregulated genes have annotated roles in the oxidative stress response, suggesting that this pathway may be superinduced in *FHIT* deficient cells (**Fig. 3A**). We validated the gene expression changes of a subset of these genes by quantitative RT-PCR (qRT-PCR) (**Fig. 3B**). The data indicate that, in the absence of cigarette smoke, *FHIT* loss does not significantly alter gene expression. However, a set of genes involved in the cytoprotective oxidative stress response induced by CSE is superinduced by CSE when *FHIT* is lost.

Table 3. Gene expression changes in response to treatment with 1% CSE in *siFHIT* treated HBEC3-TK cells

Gene assignment	Gene symbol	Gene description	p-value	Fold change: *siFHIT* plus CSE over *siControl* no CSE
NM_002133	HMOX1	Heme oxygenase decycling 1	8.41E-06	36.63
NM_02099	AKR1B10	Aldo-ketoreductase family 1, member B10	6.48E-06	12.62
NM_014331	SLC7A11	Solute carrier family 7	1.14E-04	6.88
NM_002061	GCLM	Glutamate-cysteine ligase, modifier subunit	3.39E-06	4.97
NM_032145	FBXO30	F-box protein 30	7.44E-07	3.29
NM_001143818	SERPINB2	Serpin peptidase inhibitor, clade B, member 2	3.23E-04	3.93
NM_001354	AKR1C2	Aldo-ketoreductase family 1, member C2	4.42E-06	5.55
NM_000146	FTL	Ferritin, light polypeptide	1.09E-05	4.29
NR_033752	LOC344887	NmrA-like family domain containing 1 pseudogene	2.18E-05	8.71
NM_007034	DNAJB4	DnaJ (Hsp40) homolog, subfamily B, member 4	1.01E-05	3.35
NM_032717	AGPAT	1-acylglycerol-3-phosphate O-acyltransferase	2.06E-07	2.44
NM_080725	SRXN1	Sulfiredoxin 1	2.48E-06	2.93
NM_00330	TXNRD1	Thioredoxin reductase 1	8.43E-07	2.79
NM_006912	RIT1	Ras-like without CAAX1	1.16E-06	2.91
NM_001498	GCLC	Glutamate-cysteine ligase, catalytic subunit	1.49E-05	2.72
NM_003714	STC2	Stanniocalcin 2	2.06E-05	2.79
NM_003359	UGDH	UDP-glucose 6-dyhydrogenase	2.53E-06	2.35
NM_000104	CYP1B1	Cytochrome P450, family 1, subfamily B	1.44E-04	3.81
NM_003739	AKR1C3	Aldo-ketoreductase family 1, member C3	3.45E-04	3.51
NM_012124	CHORDC1	Cysteine and histidine-rich domain (CHORD)-containing 1	2.97E-05	1.80
NM_021127	PMAIP1	Phorbol-12-myristate-13-acetate-induced protein 1	1.73E-04	2.06
NM_006470	TRIM16	Tripartite motif-containing 16	3.17E-04	1.94
NM_012328	DNAJB9	DNAJ (Hsp40) homolog, subfamily B, member 9	1.47E-04	2.45
NM_001037330	TRIM16L	Tripartite motif-containing 16-like	3.46E-07	2.21
NM_002359	MAFG	v-maf musculoaponeurotic fibrosarcoma oncogene homolog G (avian)	5.23E-04	2.21
NM_022060	ABHD4	Abhydrolase domain containing 4	8.89E-06	2.22
NM_014220	TM4SF1	Transmembrane 4 L 6 family member 1	1.03E-04	1.88
NM_001432	EREG	Epiregulin	3.28E-05	2.05
NM_021963	NAP1L2	Nucleosome assembly protein 1-like 2	5.24E-04	1.80
NM_031412	GABARAPL1	GABA(A) receptor-associated protein like 1	2.86E-04	2.27
NM_018252	TMEM206	Transmembrane protein 206	2.24E-04	1.95
NM_001080493	ZNF823	Zinc finger protein 823	3.03E-05	2.45
NM_018169	C12orf35	Chromosome 12 open reading frame 35	2.50E-05	1.53
NM_001102429	ZFAND4	Zinc finger, AN1-type domain 5	1.56E-04	1.80
NM_002083	GPX2	Glutathione peroxidase 2	5.66E-05	3.05
NM_002032	FTH1	Ferritin, heavy polypeptide	3.30E-07	1.97
NM_013390	TMEM2	Transmembrane protein 2	2.29E-06	3.07
NM_000903	NQO1	NADPH dehydrogenase, quinone 1	1.91E-07	2.12
NM_003900	SQSTM1	Sequestome 1	1.98E-04	2.23
NM_080632	UPF3B	UPF3 regulator of nonsense transcripts homolog B (yeast)	9.18E-05	1.64
NM_021187	CYP4F11	Cytochrome P450, family 4, subfamily F, polypeptide 11	9.87E-05	2.03
NM_182485	CPEB2	Cytoplasmic polyadenylation element binding protein 2	1.34E-04	1.81
NM_014117	C16orf72	Chromosome 16 open reading frame 72	6.56E-04	1.74
NM_014518	ZNF229	Zinc finger protein 229	3.84E-04	1.71
NM_002603	PDE7A	Phosphodiesterase 7A	6.83E-04	1.82
NM_004346	CASP3	Caspase 3, apoptosis-related cystein polypeptide	1.54E-04	1.63
NM_013370	OSGIN1	Oxidative stress induced growth inhibitor 1	7.05E-04	1.81
NM_181659	NCOA3	Nuclear receptor coactivator 3	8.15E-06	1.87
NR_027405	MTHFD2	Methylenetetrahydrofolate dehydrogenase (NADP+ dependent)	1.65E-04	1.58
NM_014743	KIAA0232		6.37E-07	2.38
NM_018047	RBM22	RNA binding motif protein 22	2.63E-04	1.63
NM_001912	CTSL1	Cathepsin L1	4.01E-05	1.93
NM_017853	TXNL4B	Thioredoxin-like 4B	2.04E-04	1.80
NM_001146108	PTGR1	Prostaglandin reductase 1	3.34E-04	1.56
NM_003043	SCL6A6	Solute carrier family 6	9.87E-06	1.92
NM_005080	XBP1	X-box binding protein 1	6.23E-04	1.58
NM_173601	GXYLT1	Glucoside xylotransferase 1	4.54E-04	1.84
NM_001145045	ZNF286B	zinc finger protein 286B	1.13E-04	1.86
NM_018259	TTC17	tetratricopeptide repeat domain 17	1.79E-04	1.56
NM_020772	NUFIP2	nuclear fragile X mental retardation protein interacting protein	8.91E-06	1.53

(*continued on next page*)

Table 3. Gene expression changes in response to treatment with 1% CSE in *siFHIT* treated HBEC3-TK cells (Continued)

Gene assignment	Gene symbol	Gene description	p-value	Fold change: *siFHIT* plus CSE over *siControl* no CSE
NM_020928	ZSWIM6	zinc finger, SWIM-type containing 6	1.54E-04	1.62
NM_001012661	SLC3A2	solute carrier family 3 (activators of dibasic and neutral am	6.21E-05	1.67
NR_026562	C20orf24	Chromosome 20 open reading frame 24	7.56E-04	1.58
NM_015971	MRPS7	mitochondrial ribosomal protein S7	1.76E-04	1.50
NM_018566	YOD1	YOD1 OTU deubiquinating enzyme 1 homolog (S. cerevisiae)	3.06E-05	1.91
NM_005734	HIPK3	Homeodomain interacting protein	5.14E-04	1.63
NM_018403	DCP1A	DCP1 decapping enzyme homolog A	8.23E-04	2.28
NM_001353	AKR1C1	Aldo-ketoreductase family 1, member C1	5.74E-04	1.74
NM_001135643	DCTN4	Dynactin 4	7.34E-04	1.69
NM_198965	PTHLH	Parathyroid hormone-like hormone	5.11E-05	1.71
NM_001031617	COX19	Cytochrome c oxidase assembly homolog	4.35E-04	1.59
NM_004973	JARID2	Jumonji, AT rich interactive domain 2	8.27E-05	1.57
NM_001949	E2F3	E2F transcription factor 3	2.63E-04	2.01
NM_018941	CLM8	Ceroid-lipfuscinosis, neuronal 8	5.89E-04	1.65
NM_001099270	DICER1	Dicer 1, ribonuclease type III	6.27E-05	1.71
NM_006154	NEDD4	Neural precursor cell expressed, developmentally downregulated 4	7.23E-04	1.52
NM_005017	PCTY1A	Phosphate cytydylyltransferase 1, choline, alpha	9.91E-05	1.62
NM_016535	UBAP1	Ubiquitin associated protein 1	6.23E-04	1.53
NM_004101	F2RL2	Coagulation factor II (thrombin) receptor-like 2	1.51E-04	1.52
NM_181453	GCC2	GRIP and coiled-coil domain containing 2	2.73E-04	1.52
NM_178819	AGPAT6	1-acylgylcerol-3-phosphate O-acyltransferase 6	2.54E-04	1.63
NM_017921	NPLOC4	Nuclear protein localization 4 homolog	7.51E-05	1.67
NM_024852	EIF2C3	Eukaryotic transcription initiation factor 2C, 3	8.33E-04	1.51
NM_015428	ZNF473	Zinc finger protein 472	3.28E-05	1.53
NM_002657	PLAGL2	Pleiomorphic adenoma gene-like 2	5.10E-05	1.61
NM_014494	TNRC6A	Trinucleotide repeat containing 6A	1.81E-06	1.78
NM_004096	EIF4EBP2	Eukaryotic translation initiation factor 4E binding protein 2	1.23E-04	1.66
NM_014822	SEC24D	SEC24 family, member D	2.24E-04	1.59
NM_198275	MPZL3	Myelin protein zero-like 3	6.88E-04	1.54
NM_014761	KIAA0174		1.83E-04	1.55
NM_004846	EIF4E2	Eukaryotic translation initiation factor 4E family member 2	3.73E-04	1.55
NM_004615	TSPAN7	Tetraspanin 7	1.15E-04	1.69
NM_003071	HLTF	Helicase-like transcription factor	7.77E-04	−1.63
NM_199229	RPE	Ribulose-5-phosphate-3-epimerase	2.01E-05	−1.54
NM_020240	CDC42SE2	CDC42 small effector 2	4.65E-05	−1.62
NM_017858	TIPIN	TIMELESS interacting protein	5.77E-04	−1.52
NM_001004301	ZNF813	Zinc finger protein 813	1.34E-04	−1.81
NM_000064	C3	Complement component 3	2.45E-05	1.70
NM_000435	SNCA	Synuclein, alpha (non A4 component of amyloid precursor)	7.55E-04	−1.5
NM_001037540	SCML1	Sex comb on midleg-like 1	6.77E-04	−1.64
NM_016133	INSIG2	Insulin induced gene 2	3.25E-05	−1.75
NM_002894	RBBP8	Retinoblastoma binding protein 8	6.89E-06	−1.76
NM_032438	L2MBTL3	L(3)mbt-like 3 (Drosophila)	1.77E-04	−1.65
NM_003534	HIST1H3G	Histone cluster 1, H3g	4.01E-04	−1.73
NM_182909	FILIP1L	Filamin A interacting protein-like	1.45E-04	−1.64
NR_027244	LOC151009	Hypothetical LOC151009	4.11E-04	−1.69
NM_002065	GLUL	Glutamate-ammonia ligase	4.33E-04	−1.53
NM_020529	NFKBIA	Nuclear factor of kappa light polypeptide gene enhancer in B-cell	1.47E-05	−1.58

Hmox1 expression is enhanced by *FHIT* knockdown in CSE stressed cells

One of the CSE-induced genes that is superinduced in *FHIT* knockdown cells is *HMOX1*. *HMOX1* is a member of a battery of stress response genes whose expression is controlled, in part, by promoter stress response elements.[39,51-53] We validated the upregulation of Hmox1 observed in the microarray experiment by qRT-PCR (**Fig. 4A**). In the absence of CSE, *HMOX1* mRNA is present in amounts approaching the threshold of qRT-PCR detection and the protein is undetectable by western blot (**Fig. 4A, B**). CSE treatment induces *HMOX1* mRNA and protein expression to readily detectable levels (**Fig. 4A, B**). CSE exposure combined with *FHIT* knockdown markedly increases the level of Hmox1 protein (**Fig. 4B**). There are at least 2 heme oxygenase isoforms in mammals, *HMOX1* and *HMOX2*. While *HMOX2* is expressed constitutively and confers protection to basal levels of oxidation, *HMOX1* is strictly induced in response to stress.[40,54,55] Thus, the expression pattern we detected in HBEC3-TK cells is normal. To ascertain that the increase in *HMOX1* is not due to an off-target effect of one of the siRNAs,

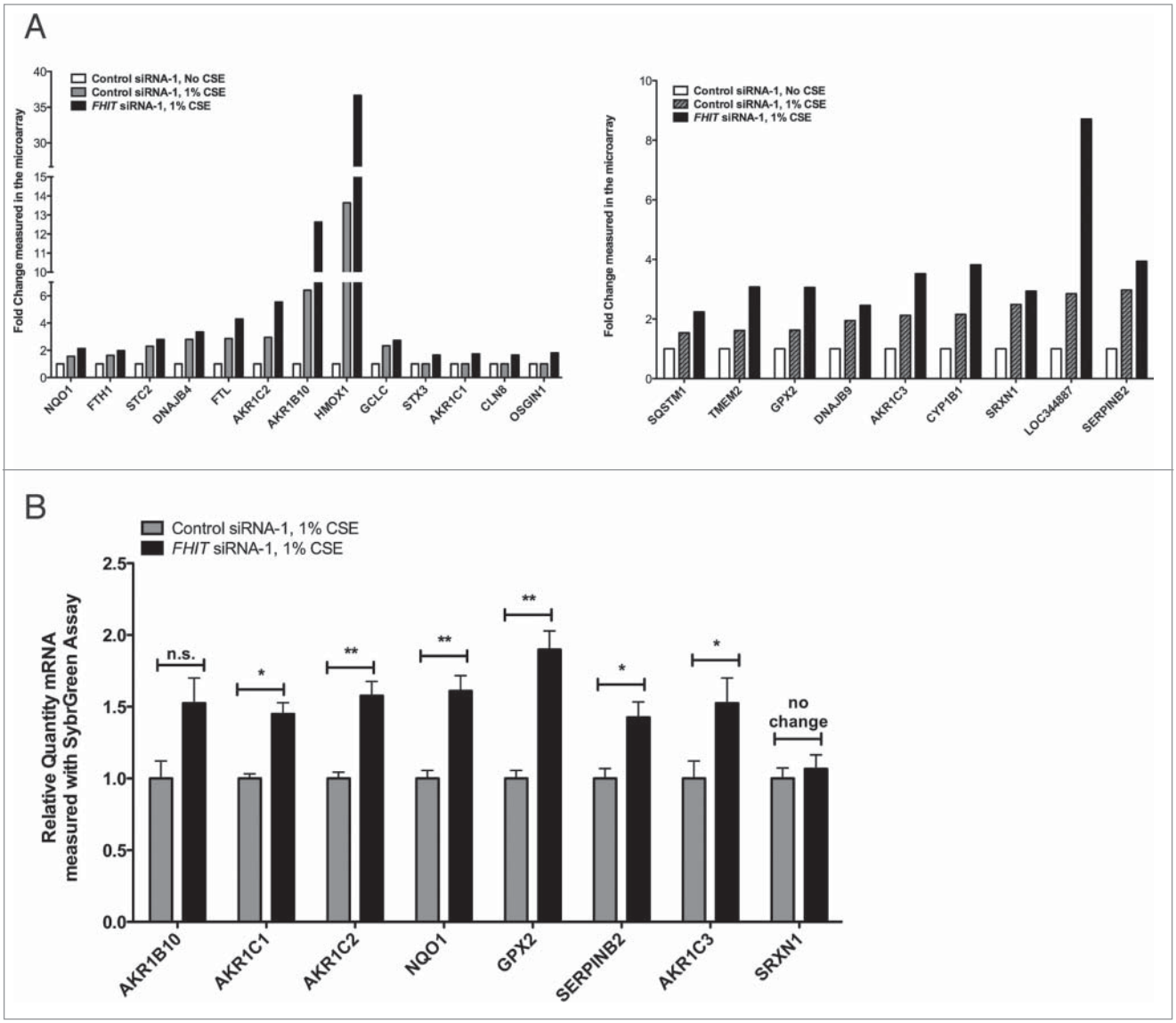

Figure 3. *FHIT* knockdown enhances expression of oxidative stress response genes after cigarette smoke treatment. HBEC3-TK cells were transfected with control or *FHIT*-targeting siRNAs for 48 hours. Cells were then exposed to 1% CSE for 4 hours or were left untreated. (**A**) Gene expression after siRNA treatment was analyzed with microarray. The left panel demonstrates that enhanced expression of a set of oxidative stress response genes was detected in *FHIT* knockdown cells after exposure to 1% CSE. All of the genes in this set pass FDR correction after ANOVA, $P \leq 0.05$. The right panel demonstrates enhanced expression of genes in *FHIT* knockdown cells. In these cases, upregulation passed FDR in *FHIT* knockdown cells but did not pass this statistical screen in siControl treated cells. (**B**) qRT-PCR validation of the microarray data. Data represent the results of at least three independent experiments. A 2-tailed paired t-test was used to assess significance of the data; $*P \leq 0.05$; $**P \leq 0.01$. Error bars represent standard deviations.

we transfected cells in parallel with a second control and second *FHIT*-targeting siRNA. In doing so, we confirmed that the increase in *HMOX1* is due to *FHIT* loss (**Fig. 4B**). Importantly, the induction of *HMOX1* is not affected by the transfection procedure, as indicated by the equivalent results in cells treated with control siRNA and those not treated with siRNA (**Fig. 4B**). These data indicate that in the presence of CSE, *FHIT* knockdown superinduces *HMOX1* expression.

To confirm that the *FHIT* knockdown-mediated enhancement of *HMOX1* induction is not unique to HBEC3-TK cells, we replicated the experiment in 2 unrelated cell lines. We first used an immortalized tracheal airway epitheial cell line, TERT-T106.[20,41] In these cells, *HMOX1* is not detected in the absence of CSE (**Fig. 5A**). As observed in HBEC3-TK cells, Hmox1 protein expression is induced by CSE and superinduced when *FHIT* is knocked down (**5A**). We then tested if the effect was present in immortalized human foreskin keratinocytes (TERT-HFK)[20,29,31,42,56] and obtained an equivalent result (**Fig. 5B**). These findings indicate that the role of *FHIT* in limiting Hmox1 expression is not dependent on a specific genetic background or unique cell type.

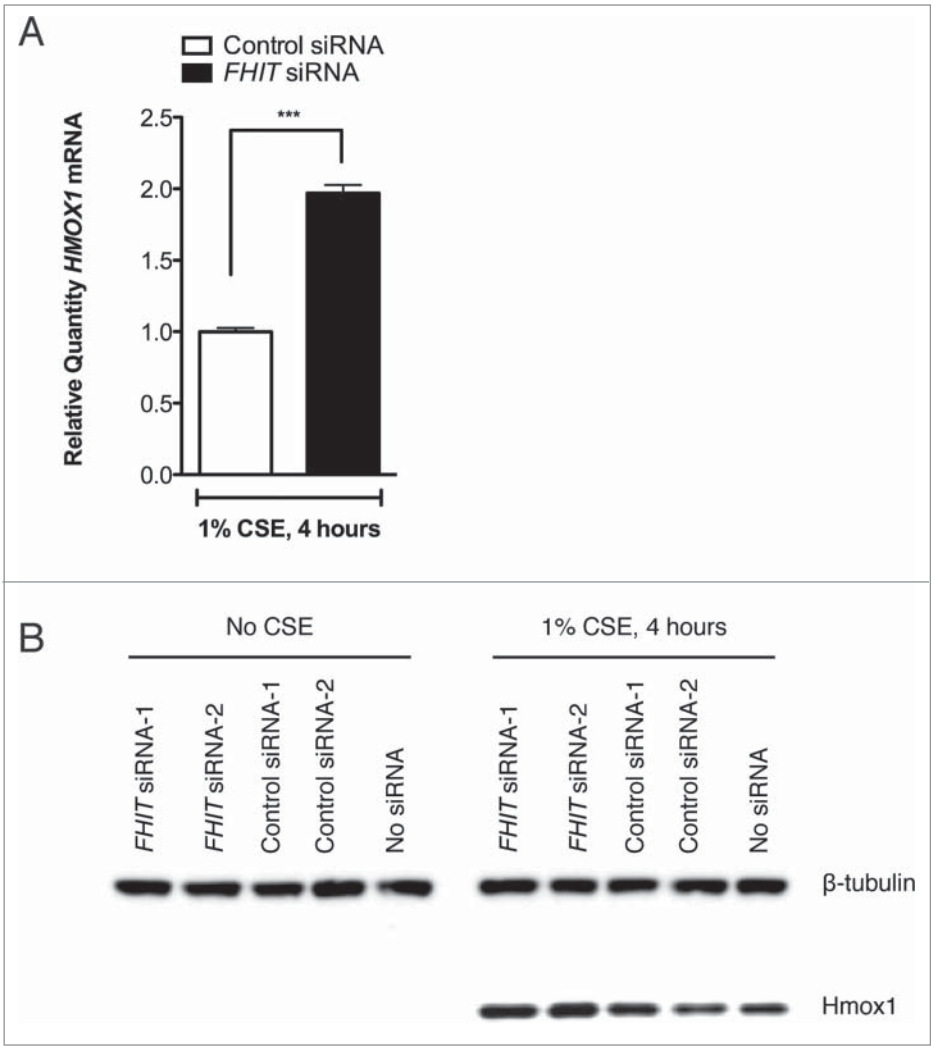

Figure 4. *FHIT* knockdown enhances the expression of *HMOX1* after cigarette smoke. HBEC3-TK cells were transfected with control or *FHIT*-targeting siRNAs. After transfection, cells were either treated for 4 hours with 1% CSE or were left untreated. (**A**) *HMOX1* was quantified by qRT-PCR. Data represent results of 6 independent experiments. A 2-tailed paired t-test was used to assess significance; ***$P \leq 0.001$. (**B**) Hmox1 protein abundance was assessed by western blot. Treatment with 2 *FHIT*-targeting siRNAs increases Hmox1 expression relative to cells treated with 2 negative control siRNAs. Western blot data are representative of 4 independent experiments.

Hmox1 induction occurs earlier and is more sustained in *FHIT* knockdown cells

To determine whether *FHIT* knockdown modulates the kinetics of protein accumulation, we exposed siRNA-treated HBEC3-TK cells to CSE for different time intervals and measured the level of Hmox1 by western blot. Hmox1 protein is detected earlier in *FHIT* knockdown cells and, consistent with previous results, is superinduced at the protein level (**Fig. 6A**). Typically, Hmox1 levels increase in response to an acute stress. Once the stress is removed, Hmox1 levels return to baseline. To test if *FHIT* knockdown affects the rate at which Hmox1 levels decay, we exposed siRNA-treated HBEC3-TK cells to 1% CSE for 4 hours and allowed the cells to recover in fresh media for various time intervals. Loss of *FHIT* increases expression of Hmox1 at each time point, but the rate of protein decay was not altered (**Fig. 6B**).

Mechanism of Hmox1 superinduction in response to *FHIT* loss

Previous studies have demonstrated that *FHIT* expression affects calcium signaling, attenuates NF-κB signaling, and promotes phosphorylation and activation of AKT.[43-45,57] Notably, modulation of these pathways has also been demonstrated to affect *HMOX1* expression.[51-53,58-60] For this reason, we asked whether the superinduction of *HMOX1* seen after *FHIT* knockdown might be mediated through one or more of these pathways. However, we found that these pathways do not contribute to upregulation of *HMOX1* in our model (**Figs. 7–10**).

Upon excluding these pathways, we analyzed the regulation of the well-characterized Bach1-Nrf2 oxidative stress response axis. Nrf2 and Bach1 are canonical regulators of *HMOX1* transcription that bind DNA *cis*-elements to activate or repress target gene transcription, respectively.[54,55,61] We found that Nrf2 mRNA and protein levels are unchanged in response to *FHIT* knockdown in both CSE treated and untreated cells (**Fig. 11A and B**). Additionally, while knockdown of *NFE2L2*, the gene that encodes Nrf2, blunts the induction of *HMOX1* in response to stress, simultaneous knockdown of *FHIT* and *NFE2L2* still yields a superinduction of *HMOX1* (**Fig. 11C**). These data indicate that the ability of *FHIT* to dampen *HMOX1* expression does not require Nrf2.

As with Nrf2, *BACH1* mRNA levels were not dependent on *FHIT* expression or the application of CSE (**Fig. 12A**). In addition, Bach1 protein levels were unchanged in response to *FHIT* knockdown in the absence of stress (**Fig. 12B**). However, two observations about Bach1 protein were made in CSE-treated cells. First, CSE treatment produced a slowly migrating species of Bach1 (**Fig. 12B**). This species was confirmed to be Bach1 by siRNA knockdown in an independent experiment (**Fig. 12C**). Second, the total level of Bach1 protein was decreased in *FHIT* knockdown cells. Quantification of the results of multiple experiments indicates that *FHIT* knockdown combined with CSE stress results in a ~40% reduction in Bach1 protein (**Fig. 12D**). To test whether a reduction in Bach1 is sufficient to induce

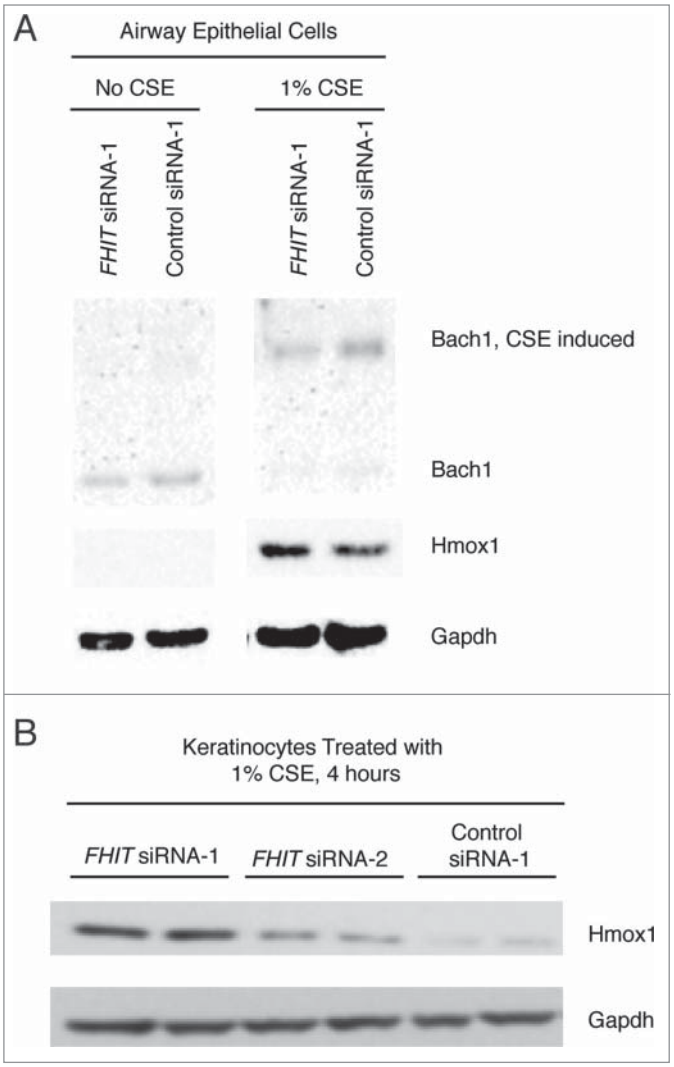

Figure 5. *FHIT* loss enhances Hmox1 expression in TERT-HFK and TERT-T-106 cells. (**A**) Human foreskin keratinocytes or (**B**) tracheal airway epithelial (T106) cells were transfected with control or *FHIT*-targeting siRNAs. After knockdown, cells were exposed to 1% CSE for 4 hours. Hmox1 protein abundance was assessed by western blot. The data show that Hmox1 expression is enhanced by *FHIT* knockdown in these cells, demonstrating that the role of *FHIT* in modulating Hmox1 expression does not require a specific genetic background.

Hmox1 protein, we titrated *BACH1* siRNA into HBEC3 cells and saw a clear and inverse relationship between Bach1 and Hmox1 levels (**Fig. 13A and B**). Interestingly, we also note that the levels of Fhit and Bach1 protein are inversely correlated. Taken together, the data indicate that the superinduction of *HMOX1* in *FHIT* knockdown cells may be mediated through decreased stability or translation of Bach1 protein in cells that have both lost *FHIT* and are stressed with cigarette smoke.

Discussion

This work provides evidence of a role for *FHIT* in the cellular response to oxidative stress, demonstrating that when *FHIT* is depleted from cells exposed to cigarette smoke, the induction of a subset of oxidative stress response genes, including *HMOX1*, is enhanced. Several studies have illustrated a key role for *HMOX1* in promoting cell survival during inflammation, and *HMOX1* expression has multiple functions in smoking-mediated lung cancers.[20,62-65] Because *HMOX1* promotes cell proliferation and increases resistance to oxidative stress, overexpression of *HMOX1* imparts a selective advantage to cells in the early stages of carcinogenesis and correlates with resistance to many chemotherapeutics in malignancy.[20,29,31,56] Thus, our data link loss of Fhit to a key pathway in the establishment and maintenance of the malignant state.

A multitude of signaling pathways impact the expression of *HMOX1.* We investigated several implicated pathways and identified a relationship between loss of Fhit and reduced protein levels of Bach1. The Bach1 transcription factor suppresses the expression of a battery of stress response genes. In the absence of stress, Bach1 binds to DNA antioxidant response elements (AREs) and strongly represses gene transcription. Upon application of stress, Bach1 is released from DNA and is exported to the cytoplasm where it is targeted for ubiquitylation and proteasome-mediated degradation.[57] Concomitant with Bach1 export, the activating transcription factor Nrf2 translocates into the nucleus and occupies AREs previously bound by Bach1, promoting a coordinated induction of stress response genes. Aberrant transcriptional activity of Bach1 and Nrf2 underlie several diseases, including many cancers. Our study suggests that *FHIT* knockdown decreases protein levels of Bach1, which is sufficient to enhance expression of *HMOX1* in epithelial cells. An outstanding question is how *FHIT* loss leads to decreased Bach1 protein levels. Bach1 is targeted for ubiquitylation by the E3 ligase HOIL-1 (RBCK1), but to date we have not seen differences in HOIL-1 expression levels in *FHIT* knockdown relative to control treated HBEC3-TK cells, nor have we seen differences in HOIL-1 splice variants (unpublished data). Additionally, we have not detected a difference in nuclear export of Bach1 that depends on Fhit expression (unpublished results). Importantly, it is clear that *BACH1* mRNA levels are not affected by *FHIT* loss, so we hypothesize that Fhit modulates the stability or translation of Bach1 protein. Strikingly, the inverse relationship between levels of Fhit and Bach1 protein implies that the *FHIT* gene may be a target of repression by Bach1. This finding is interesting as it suggests that the proteins participate in a regulatory feedback loop during control of the oxidative stress response in cancer-promoting environments.

Substantive evidence implicates Fhit in tumor suppression but the precise mechanism underlying the function has not been elucidated. Fhit protein is a dimeric histidine triad protein that binds and hydrolyzes diadenosine triphosphate (ApppA) and related nucleotides.[58-60] ApppA, a product of reactions catalyzed by tRNA synthetases and other enzymes, has been proposed to have several intracellular functions including signaling stress responses.[61] Indeed, the intracellular concentration of ApppA increases in cells exposed to oxidative stressors.[62-65] Because mutation of the Fhit enzyme active site histidine residue greatly retards ApppA cleavage without a strong effect on ApppA binding or proapoptotic activity

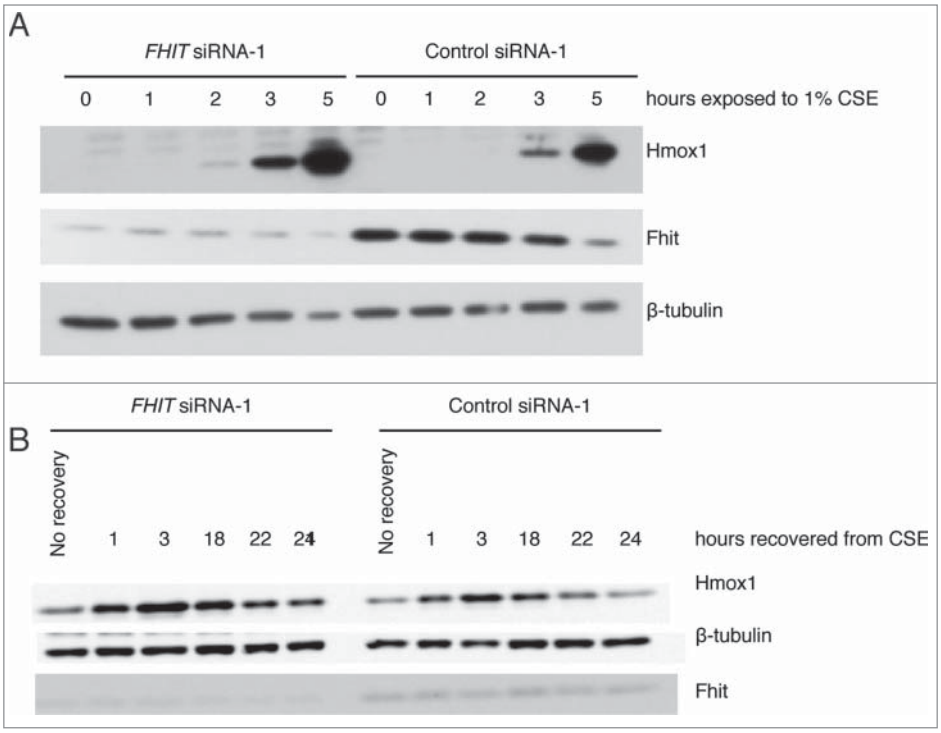

Figure 6. *FHIT* knockdown induces early and sustained expression of Hmox1. HBEC3-TK cells were transfected with control or *FHIT* siRNAs and exposed to 1% CSE for increasing time points, up to 4 hours. After 4 hours, cells were recovered in fresh media for increasing amounts of time. (**A**) Hmox1 protein is detected earlier in *FHIT* knockdown cells and (**B**) Hmox1 expression is enhanced at all time points by *FHIT* loss. Data represent the results of three independent experiments. At each time point, there is approximately 2-fold greater Hmox1 in *FHIT* knockdown cells.

in a reexpression assay, it has been argued that the Fhit-ApppA complex may mediate the function of Fhit.[2,66-68] While these experiments were valuable in dissection of the amino acids and nucleotide interactions linked to Fhit function, the Fhit re-expression system may have biased the result to an apoptotic pathway. In contrast, our model recapitulates the process of carcinogenesis by analyzing the cellular consequence of *FHIT* loss. It will be interesting to probe the relationship between CSE and induction of ApppA and related nucleotides in the control of oxidative stress genes.

Since its discovery in 1996, hundreds of papers have described the *FHIT* gene. Many of these studies attempt to dissect the mechanism of Fhit-mediated tumor suppression, but they present disparate explanations for the phenomenon, and a unifying theory has proved to be elusive. Our proposal that Fhit limits cell growth by attenuating the oxidative stress response is supported by independently published studies that connect Fhit function with the accumulation of intracellular ROS. For example, *FHIT*-deficient bone marrow cells (BMC) have lower levels of ROS after hydroquinone challenge. A reduction in intracellular levels of ROS are detected in *FHIT* negative BMCs relative to wild-type, and this reduction in ROS accumulation is linked to failure to induce apoptosis as the

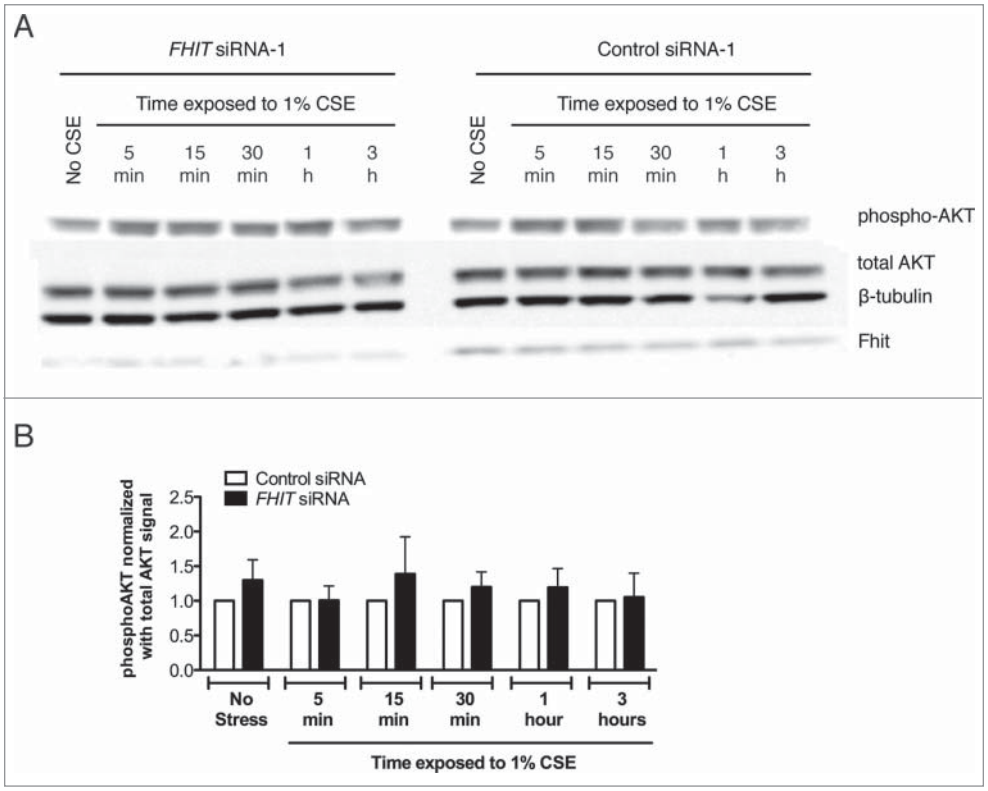

Figure 7. PI3K inhibition does not affect expression of *FHIT*. HBEC3-TK cells were treated with control or *FHIT* siRNA for 48 hours. Cells were pretreated with 30 μM LY294002 or DMSO vehicle for 1 hour and then treated with 1% CSE supplemented with 30 μM LY294002 or DMSO for the indicated time intervals. (**A**) Western blot demonstrates that *FHIT* knockdown does not affect phosphorylation of AKT. AKT is phosphorylated in response to CSE but is not altered in degree of activation by *FHIT* knockdown. (**B**) Densitometry measurements of three independent experiments. p-values were determined with a 2-tailed t-test; * $P \leq 0.05$. Error bars indicate standard deviations of triplicate samples.

phenotype is reversed with application of the antioxidant *N*-acetyl-L-cysteine.[1,5,7-9,69] Several studies that connect Fhit expression to increased sensitivity to anti-cancer drugs may also serve to substantiate the link between Fhit function and oxidative stress. Re-expression of Fhit in Fhit-negative cancer-derived cell lines increases sensitivity to mitomycin C (MMC), camptothecin (CPT), and cisplatin. [13,15,70,71] While the canonical role of each drug involves modulation of DNA topography to induce DNA damage,[16,17,72-74] each agent also effects ROS production, and the production of ROS has been demonstrated to underlie the toxic effect of each compound.[1,75-79] Resupplying *FHIT* to *FHIT*-negative cells increases cell death after MMC, CPT, and cisplatin treatments, but this phenomenon has not explained mechanistically. Thus the ability of Fhit to dampen expression of antioxidant response genes may not only explain the effects of *FHIT* gene loss in this study but the effect of *FHIT* reexpression in many studies.

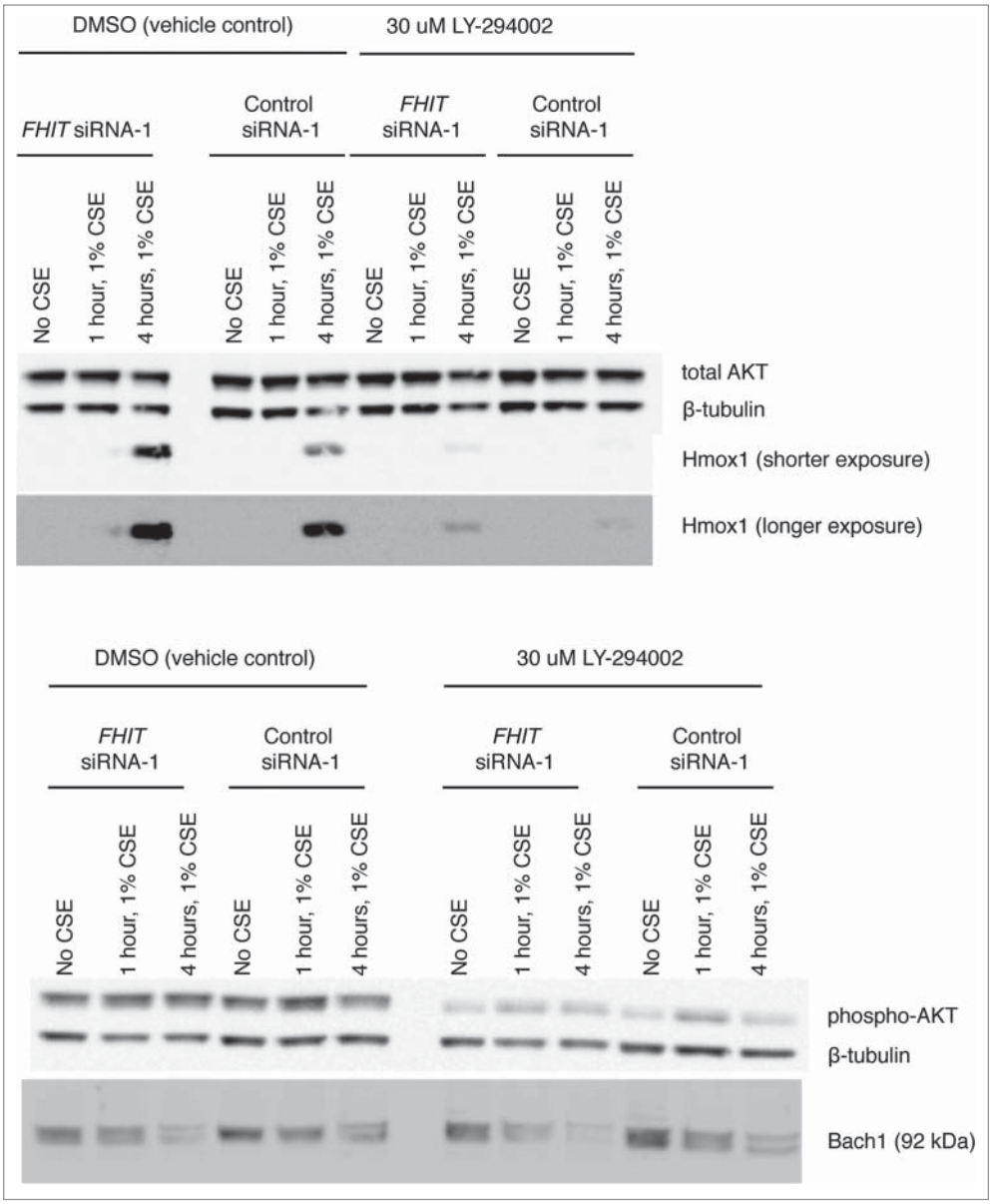

Figure 8. PI3K inhibition blunts the induction of Hmox1 but does not effect *FHIT* mediated repression of Hmox1. Treatment with LY294002 inhibits phosphorylation of AKT and blunts induction of Hmox1 in response to CSE. Hmox1 remains superinduced in *FHIT* knockdown cells.

Materials and Methods

Cell culture

HBEC3-TK bronchial epithelial cells were a kind gift from Dr. John Minna (UT Southwestern). TERT-HFK human foreskin keratinocytes and TERT-T106 tracheal airway epithelial cells were generous gifts of Dr. Aloysius Klingelhutz (University of Iowa). Cells were cultured on bovine collagen coated plastic dishes (Sigma, Cat #C4243). Cells were maintained in Keratinocyte Serum Free Media (KSFM) supplemented with BPE (12.5 g/ml) and EGF (5.0 ng/ml) (Gibco Cat #17005-075). Cells were grown in humidified 37°C, 5% CO_2 incubators.

siRNA transfection

Cells were seeded at densities of 400,000 cells/plate (10 cm dishes), 125,000 cells per well (6 well dishes), or 30,000 cells/well (12 well dishes). After overnight incubation, cells were transfected with 15 nM siRNA and Lipofectamine RNAiMax (Invitrogen, Carlsbad CA) according to the manufacturer's protocol. siRNAs were obtained from commercial vendors. *FHIT* siRNA-1 (Cat #4390843), *FHIT* siRNA-2 (Cat #AM16706), Control siRNA-1 (Cat #4390843), and Control siRNA-2 (Cat #4390846) were purchased from Ambion (Life Technologies). *BACH1* siRNA (Cat # HSC.RNAI.N001186.12.1) and *NFE2L2* siRNA (Cat #HSC.RNAI.N001145412.12) were purchased from IDT (Coralville, IA). After 4.5 hours of siRNA incubation, transfection media were replaced with fresh KSFM. Cells were incubated for 48 hours.

Cigarette smoke extract preparation

Research grade cigarettes were purchased from the University of Kentucky. After removing the filter, the cigarette was

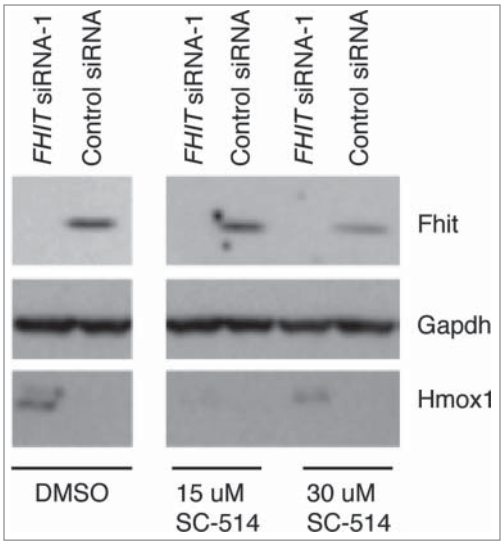

Figure 9. NFkB inhibition blunts the induction of Hmox1 but does not effect *FHIT*-mediated repression of Hmox1. SC-514 is a selective inhibitor of IKK2 and blocks NF-kB dependent gene expression. HBEC3-TK cells were treated with control or *FHIT* siRNA for 48 hours. Cells were pre-treated with 15 μM SC-514, 30 μM SC-514, or DMSO vehicle for 2 hours. Cells were then treated with 1% CSE supplemented with DMSO vehicle or indicated concentrations of SC-514. Western blot was used to detect levels of Hmox1 in the samples. While IKK2 inhibition blunts the induction of Hmox1, the protein is still superinduced in *FHIT* knockdown cells.

combusted and smoke extracted into 10 ml of KSFM, as described previously.[15,34] This preparation was termed "100% CSE." The extract was filtered though a 0.22 μm pore membrane (Millipore Cat #SCGP00525). CSE was diluted to 1% in KSFM and added to cells in culture for the indicated times. CSE treated cells were incubated separately from non-CSE treated cells.

RNA extraction, cDNA synthesis, and RT-PCR analysis

Total RNA was extracted from cells using the RNeasy Mini kit (Qiagen, Cat #74104) after homogenizing cells with Qiashredder spin columns (Qiagen, Cat #79654). RNA was DNase treated with the Turbo DNA-free kit (Ambion, Cat #AM1907). 500 ng total RNA was reverse transcribed with the iScript cDNA synthesis kit (BioRad, Cat #170–8890) or 1.5 μg total RNA was reverse transcribed with the High Capacity cDNA synthesis kit (Applied Biosystems, Cat #4368814). RT-PCR was performed with iQ SYBR Green Supermix (BioRad, Cat #170–880) and designed primers or with TaqMan Gene Expression Master Mix (Applied Biosystems, Cat #4369016) and PrimeTime nuclease primer/probe assays (IDT). Nuclease assays used in this study are: *NFE2L2*, IDT Catalog Hs.PT.49a.36704, *GAPDH*, IDT Catalog Hs.PT.47.1164609, *FHIT*, IDT Catalog Hs.PT.47.3317107, and *HMOX1*, IDT Catalog Hs.PT.53a.22439609. Primers used in SYBR Green assays are listed in 5'-3' direction as follows: *AKR1B10* – GCCACAGGGATTCAAGTCT and CTTTCACCAGCCCCTCATC; *AKR1C1* – GCCGTGGAGAAGTGTAAAGATG and CTGGTTGAAGTAAGGATGACATTC; *AKR1C2* – TAAAGCCAGGTGAGGAAGTG and CTGTGGTTGAAGTTGGACAC; *AKR1C3* - AACAAGCCAGGACTCAAGTAC and CAGAGCACTATAGGCAACCAGl *NQO1* – CCGCAGACCTTGTGATATTCC and ACTCGCTCAAACCAGCCTTTCAGA; *GPX2* – GCTTCCCTTGCAACCAATTTG and TTCTGCCCATTCACCTCAC; *SERPINB2* – CAGTAGACTTCCTAGAATGTGCAG and AAGTAGACAGCATTCACCAGG; *SRXN1* – CAAGGTGCAGAGCCTCG and CTTTGATCCAGAGGACATCGA; *BACH1* – TCTTGAATCAGAAATTGAGAAGCTG and TGGCAAAGTCCAGTTAGGTTCTGCT; *GAPDH* – ACATCGCTCAGACACCATG and TGTAGTTGAGGTCAATGAAGGG.

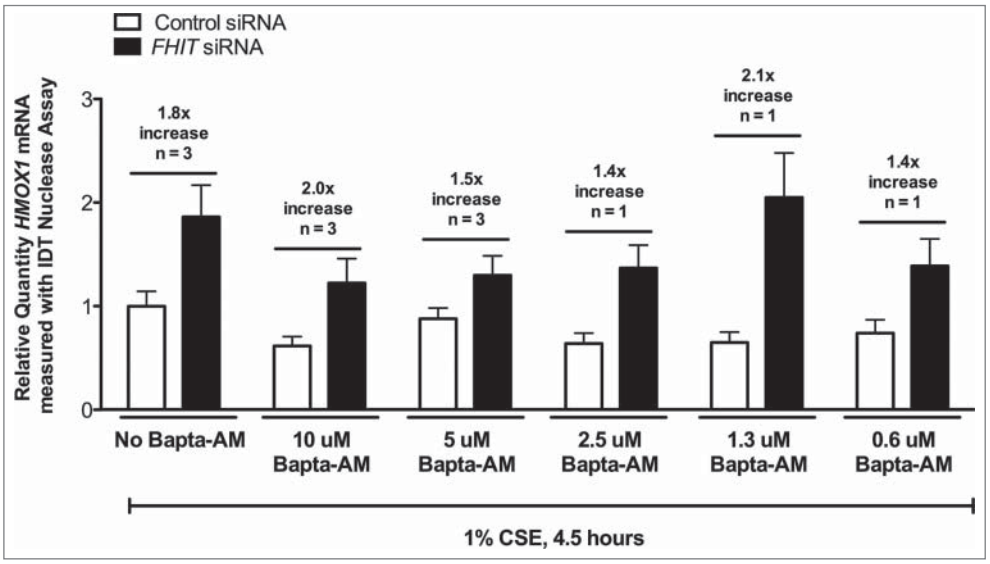

Figure 10. Calcium chelation does not affect *FHIT*-mediated repression of *HMOX1*. HBEC3-TK cells were treated with control or *FHIT* siRNA for 48 hours. Cells were treated with DMSO vehicle, 10 μM BAPTA-AM, or 5 μM BAPTA-AM for 30 minutes. Cells were then treated with 1% CSE for 4.5 hours. qRT-PCR was used to detect *HMOX1* expression in the cells. While BAPTA-AM blunts the induction of *HMOX1* in response to CSE, *HMOX1* expression is still superinduced by *FHIT* knockdown.

Immunoblotting

Cells were suspended in ice-cold RIPA buffer (50 mM Tris-Cl (pH 8), 1% NP-40, 0.5% Na deoxycholate, 0.1% SDS, 150 mM NaCl, 5 mM EDTA) supplemented with protease inhibitors (Roche Cat #11836170001) and phosphatase inhibitors (Roche Cat #04906845001). Cells were lysed on ice for 20 minutes before clarifying (4°C, 13 K rpm, 10 minutes). Protein content was quantified with the BCA Protein Assay (Pierce Cat #23225). Equivalent amounts of protein were reduced with 50 mM DTT, denatured with LDS, heated,

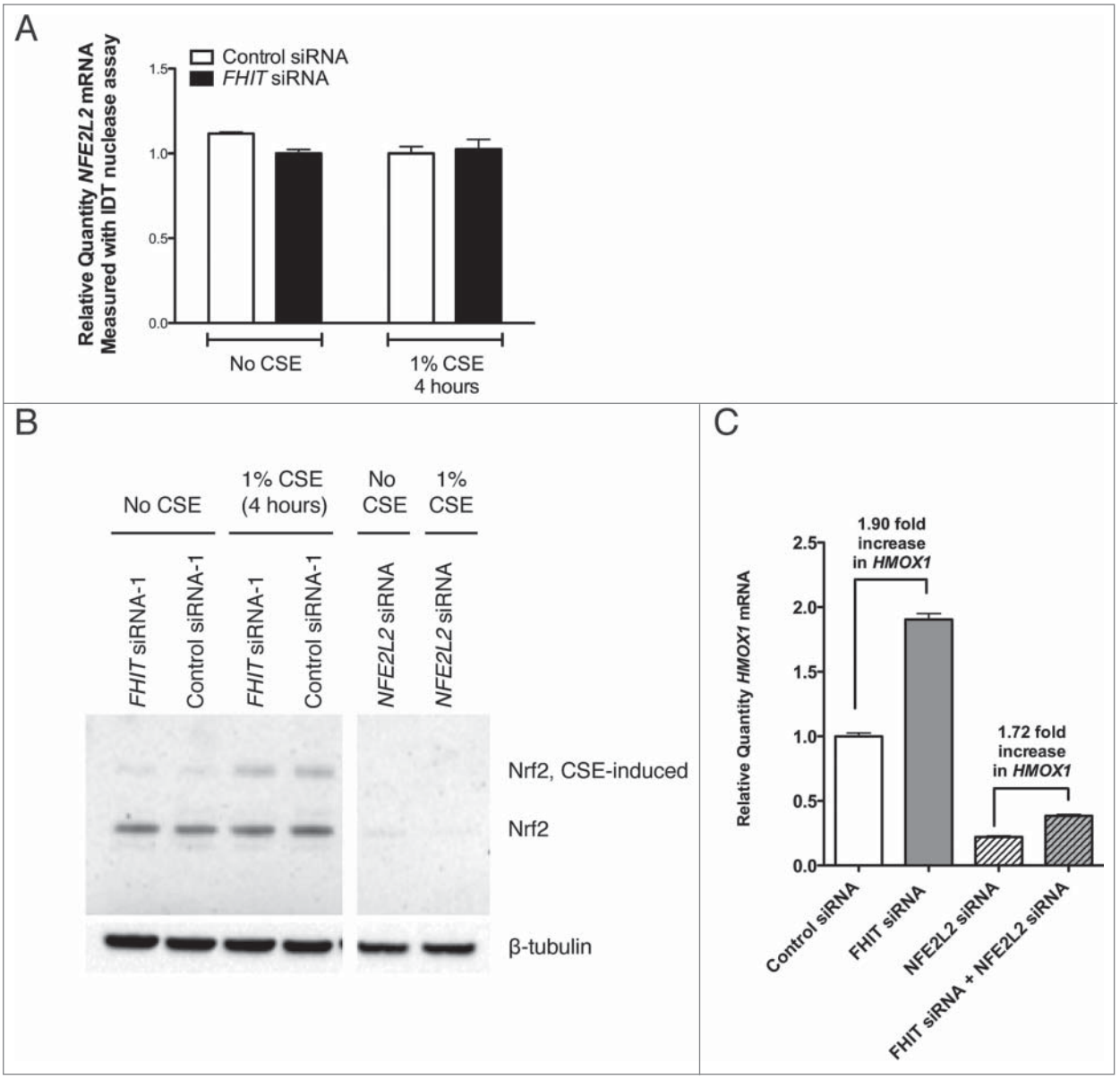

Figure 11. *FHIT*-mediated repression of *HMOX1* does not require Nrf2. HBEC3-TK cells were transfected with control, *FHIT*, or *NFE2L2* siRNAs. After transfection, cells were either treated for 4 hours with 1% CSE or left untreated. (**A**) *NFE2L2* (Nrf2) expression was quantified by qRT-PCR. *FHIT* knockdown does not effect *NFE2L2* mRNA levels before or after CSE treatment. The data represent the results of three independent experiments. (**B**) Nrf2 protein abundance was assessed by protein gel blot. Nrf2 migrates at the expected molecular weight in both CSE and non-CSE treated samples. A slow migrating species of Nrf2 (~ 75 kD) appears in CSE treated cells. Treatment with *NFE2L2* siRNA confirms both isoforms as Nrf2. *FHIT* knockdown has no effect on Nrf2 protein abundance. (**C**) RNA was collected from cells transfected with control, *FHIT* siRNA, or *NFE2L2* siRNA alone, or *FHIT* and *NFE2L2* siRNA together. Knockdown of *NFE2L2* blunts the induction of *HMOX1* after CSE exposure. Concurrent knockdown of *FHIT* and *NFE2L2* yields a superinduction of *HMOX1* to a magnitude similar to that when only *FHIT* is depleted. Data represent the results of three independent experiments.

and loaded on NuPage 4–12% Bis-Tris gels (Invitrogen) and electrophoresed in 1x MOPS buffer. Protein gels were transferred to nitrocellulose membranes, which were blocked with 5% milk. Primary antibodies were incubated with membranes overnight at 4°C. Secondary antibody incubations were performed at room temperature for 30 minutes. Blots were developed with ECL - SuperSignal West Pico (Pierce), Supersignal West Femto (Pierce), or Quantum (Advansta) reagents. Images were collected with GE ImageQuant LAS4000 and quantification performed with ImageQuant TL7.0 software (GE). Fhit antibody was obtained from Millipore (Cat #07–172). Bach1 (Cat #sc-14700), Nrf2 (Cat #sc-365949), and HRP conjugated donkey-anti-goat (Cat #sc-2020) antibodies were purchased from Santa Cruz Biotechnology. Hmox1 (Cat #4643), β-tubulin (Cat #2128), Gapdh (Cat #5174), AKT (Cat #9272), phosphoAKT (Cat #4060), HRP-anti-mouse (Cat #7076), and HRP-anti-rabbit (Cat #7074) antibodies were purchased from Cell Signaling Technologies. β-actin (Cat #A2066) antibody was obtained from Sigma.

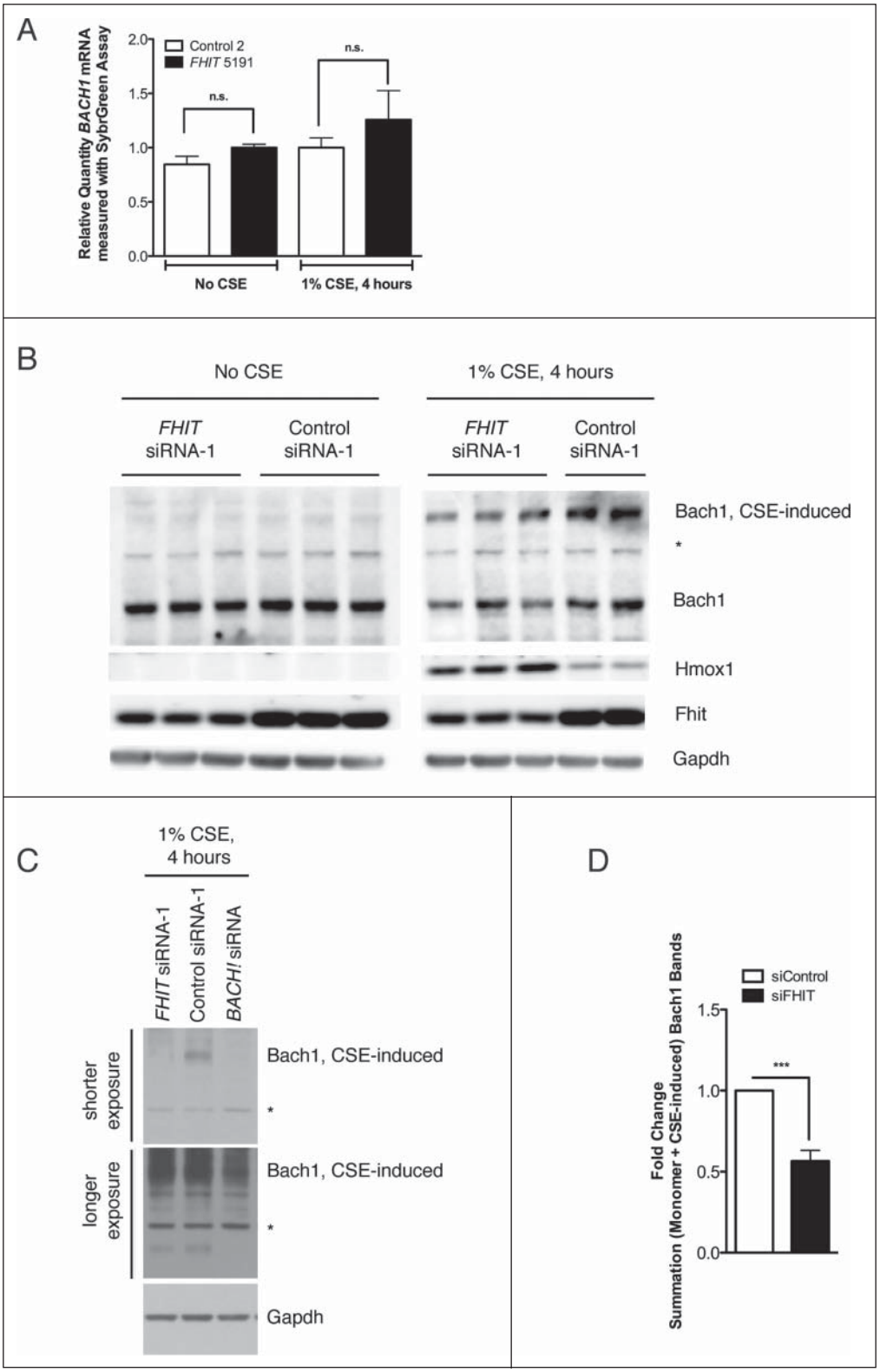

Figure 12. *FHIT* loss is associated with reduced Bach1 protein levels. HBEC3-TK cells were transfected with control or *FHIT*-targeting siRNAs. After transfection, cells were either treated with 1% CSE for 4 hours or left untreated. (**A**) *BACH1* mRNA was quantified with qRT-PCR. *FHIT* knockdown does not significantly affect *BACH1* mRNA levels before or after CSE treatment. Data represent the results of three independent experiments. (**B**) Bach1 protein abundance was assessed by western blot. Bach1 protein levels are not affected by *FHIT* knockdown in the absence of CSE. In CSE treated cells, Bach1 migrates as 2 species. A fast migrating species exists at the expected molecular weight (92 kD), and a slow migrating species exists at a higher molecular weight (~ 150 kD). Total Bach1 protein levels are reduced in *FHIT* knockdown CSE-treated cells. Western data represent the results of 4 independent experiments (**C**) *BACH1* siRNA treatment confirms both bands to be Bach1. (**D**) Relative protein quantification. Error bars represent mean +/− SEM of results from three independent experiments; $^{***}P < 0.001$.

Treatment with inhibitors

Stock solutions of inhibitors were prepared in anyhydrous DMSO, aliquoted, and stored at −20° C. Compounds were diluted to working concentrations in KSFM immediately before use. The PI3K inhibitor LY294002 was purchased from Cell Signaling Technologies (Cat #9901). The IKK2 inhibitor SC-514 was purchased from Cayman Chemical (Cat #10010267). The cell permeable Ca^{2+} chelator BAPTA-AM was purchased from Invitrogen (Cat #B-6769).

DNA microarray

Microarray hybridizations were performed at the University of Iowa DNA Facility. Briefly, 50 ng total RNA was converted to single primer isothermal amplification (SPIA) cDNA using the WT-Ovation Pico RNA Amplification System, v1 (NuGEN Technologies, San Carlos, CA, Cat #3300) according to the manufacturer's protocol. The amplified cDNA product was purified through a QIAGEN MinElute Reaction Cleanup column (QIAGEN Cat #28204) according to modifications from NuGEN. DNA product (4.0 μg) was then used to generate sense target cDNA using

the WT-Ovation Exon Module v1 (NuGEN Technologies, Cat #2000) and again cleaned up with the Qiagen column. Sense target cDNA product (5.0 μg) was fragmented (average fragment size = 85 bases) and biotin-labeled using the NuGEN FL-Ovation cDNA Biotin Module, v2 (NuGEN Technologies, Cat #4200) by the manufacturer's protocol. The biotin-labeled cDNA was mixed with Affymetrix eukaryotic hybridization buffer (Affymetrix, Inc., Santa Clara, CA) and hybridized to Affymetrix Human Gene 1.0 ST Arrays at 45°C for 18 h with 60 rpm rotation in an Affymetrix Model 640 Genechip Hybridization Oven. Following hybridization, the arrays were washed, stained with streptavidin-phycoerythrin (Molecular Probes, Inc., Eugene, OR) and with antistreptavidin antibody (Vector Laboratories, Inc., Burlingame, CA) using the Affymetrix Model 450 Fluidics Station. Arrays were scanned with the Affymetrix Model 3000 scanner (7 G upgrade) and data were collected using the GeneChip operating software v 1.4.

Microarray data analysis

The array data were analyzed for significant changes in expression using Partek Genomics Suite Software (Partek, Inc.). Three biological replicates for each treatment were processed and analyzed. Briefly, the expression value estimates generated by microarray scanners were normalized using the robust multi-array averaging algorithm. Analysis of variation followed by multiple testing correction using the false-discovery rate was used to assess significant changes in expression profile between samples. Expression data for *siControl* +/− CSE were analyzed with Ingenuity Pathway Analysis (IPA, Ingenuity Systems, www.ingenuity.com). The IPA Canonical Pathways Analysis tool was used to identify the pathways from the IPA Library of Canonical Pathways that were most significant in the data. A dataset containing gene identifiers with expression fold change and associated p-value was uploaded to the application. The data were then limited to fold change +/− 1.5 and p-value $\leq$0.05. A core analysis was performed to identify gene function and a canonical pathway analysis was used to identify the pathways to which the genes mapped. Significance is measured within IPA by 2 means: 1.) Determination of a ratio calculated by dividing the number of differentially expressed genes that map to a particular pathway by the total number of genes in that pathway; 2.) Calculation of a p-value by Fisher's exact test to determine the probability that the association between the genes in the data set and the canonical pathway can be explained by chance.

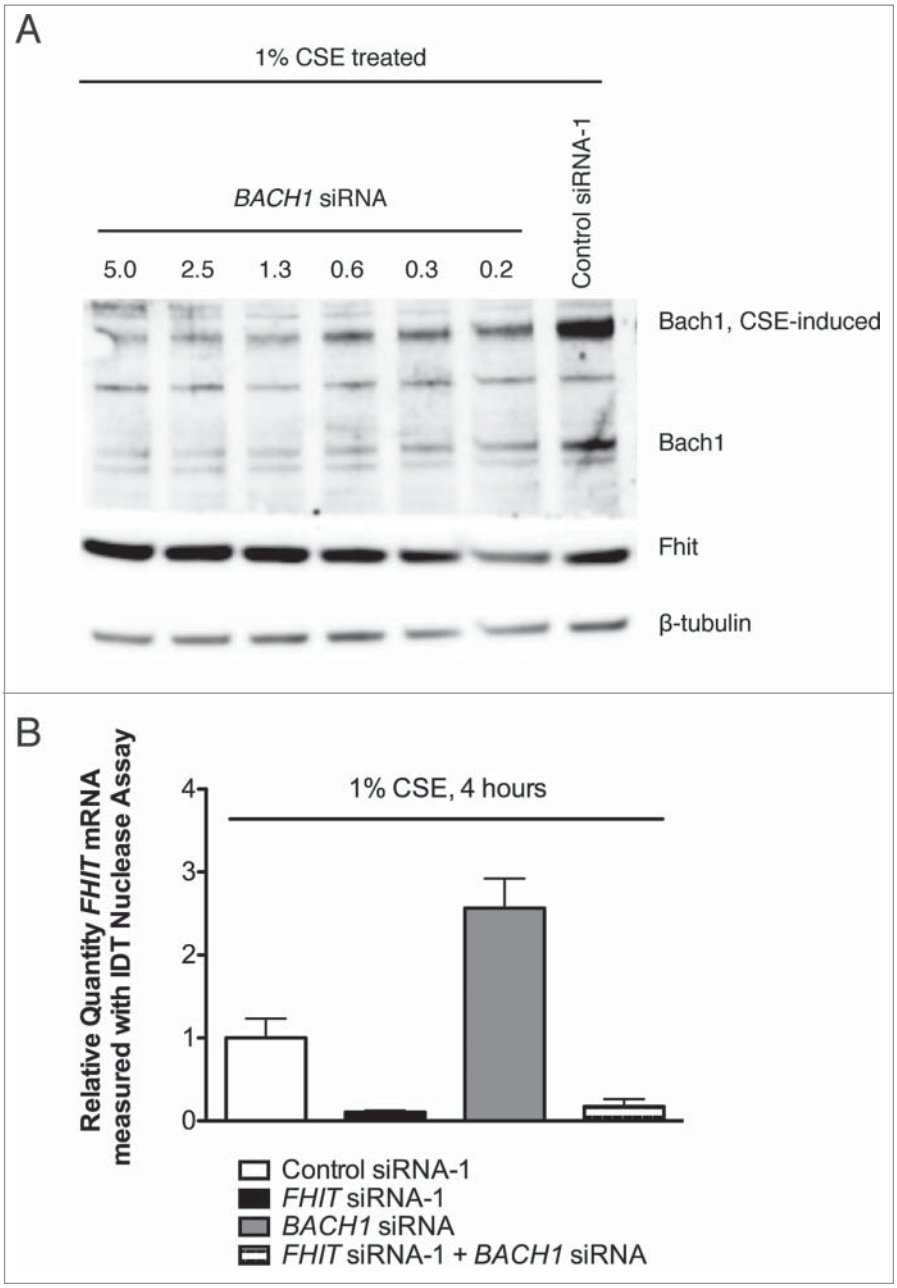

Figure 13. Fhit and Bach1 expression levels are inversely correlated. (**A**) HBEC3-TK cells were transfected with control or *BACH1* siRNA. After transfection, cells were treated with 1% CSE for 4 hours. Protein abundance was measured by western blot. Hmox1 and Fhit protein levels are inversely correlated with Bach1 protein abundance. (**B**) HBEC3-TK cells were transfected with control, *BACH1*, or *FHIT* siRNA. FHIT expression was measured by qRT-PCR. *BACH1* knockdown increases *FHIT* expression approximately 2-fold. Data represent the results of three independent experiments. Error bars represent standard deviations.

Disclosure of Potential Conflicts of Interest

No potential conflicts of interest were disclosed.

Funding

Work was supported by National Cancer Institute grant CA075954 to CB. The DNA Facility is supported by the Holden Comprehensive Cancer Center (P30CA086862).

Acknowledgments

The authors thank Drs. Kevin Knudson and Thomas Bair in the Iowa Institute of Human Genetics Genomics Division for assistance with performing and analyzing microarrays.

Supplemental Materials

Supplemental data for this article can be accessed on the publisher's website.

References

1. Zanesi N, Fidanza V, Fong LY, Mancini R, Druck T, Valtieri M, Rüdiger T, McCue PA, Croce CM, Huebner K. The tumor spectrum in FHIT-deficient mice. Proc Natl Acad Sci USA 2001; 98:10250-5; PMID:11517343; http://dx.doi.org/10.1073/pnas.191345898
2. Ohta M, Inoue H, Cotticelli MG, Kastury K, Baffa R, Palazzo J, Siprashvili Z, Mori M, McCue P, Druck T, et al. The FHIT gene, spanning the chromosome 3p14.2 fragile site and renal carcinoma-associated t(3;8) breakpoint, is abnormal in digestive tract cancers. Cell 1996; 84:587-97; PMID:8598045; http://dx.doi.org/10.1016/S0092-8674(00)81034-X
3. Dumon KR, Ishii H, Fong LY, Zanesi N, Fidanza V, Mancini R, Vecchione A, Baffa R, Trapasso F, During MJ, et al. FHIT gene therapy prevents tumor development in Fhit-deficient mice. Proc Natl Acad Sci USA 2001; 98:3346-51; PMID:11248081; http://dx.doi.org/10.1073/pnas.061020098
4. Trapasso F, Krakowiak A, Cesari R, Arkles J, Yendamuri S, Ishii H, Vecchione A, Kuroki T, Bieganowski P, Pace HC, et al. Designed FHIT alleles establish that Fhit-induced apoptosis in cancer cells is limited by substrate binding. Proc Natl Acad Sci USA 2003; 100:1592-7; PMID:12574506; http://dx.doi.org/10.1073/pnas.0437915100
5. Sozzi G, Tornielli S, Tagliabue E, Sard L, Pezzella F, Pastorino U, Minoletti F, Pilotti S, Ratcliffe C, Veronese ML, et al. Absence of Fhit protein in primary lung tumors and cell lines with FHIT gene abnormalities. Cancer Res 1997; 57(23):5207-12; PMID:9393735.
6. Sevignani C, Calin GA, Cesari R, Sarti M, Ishii H, Yendamuri S, Vecchione A, Trapasso F, Croce CM. Restoration of fragile histidine triad (FHIT) expression induces apoptosis and suppresses tumorigenicity in breast cancer cell lines. Cancer Res 2003; 63:1183-7; PMID:12649173
7. Gemma A, Hagiwara K, Ke Y, Burke LM, Khan MA, Nagashima M, Bennett WP, Harris CC. FHIT mutations in human primary gastric cancer. Cancer Res 1997; 57:1435-7; PMID:9108441
8. Petursdottir TE, Hafsteinsdottir SH, Jonasson JG, Moller PH, Thorsteinsdottir U, Huiping C, Egilsson V, Ingvarsson S. Loss of heterozygosity at the FHIT gene in different solid human tumours and its association with survival in colorectal cancer patients. Anticancer Res 2002; 22:3205-12; PMID:12530066
9. Kowara R, Golebiowski F, Chrzan P, Skokowski J, Karmolinski A, Pawelczyk T. Abnormal FHIT gene transcript and c-myc and c-erbB2 amplification in breast cancer. Acta Biochim Pol 2002; 49:341-50; PMID:12362975
10. Gao G, Kasperbauer JL, Tombers NM, Wang V, Mayer K, Smith DI. A selected group of large common fragile site genes have decreased expression in oropharyngeal squamous cell carcinomas. Gene Chromosomes Canc 2014; 53:392-401; PMID:24481768; http://dx.doi.org/10.1002/gcc.22150
11. McAvoy S, Ganapathiraju SC, Ducharme-Smith AL, Pritchett JR, Kosari F, Perez DS, Zhu Y, James CD, Smith DI. Non-random inactivation of large common fragile site genes in different cancers. Cytogenet Genome Res 2007; 118:260-9; PMID:18000379; http://dx.doi.org/10.1159/000108309
12. Hanahan D, Weinberg RA. Hallmarks of Cancer: The Next Generation. Cell [Internet] 2011; 144:646-74. Available from: http://linkinghub.elsevier.com/retrieve/pii/S0092867411001279
13. Stein CK, Glover TW, Palmer JL, Glisson BS. Direct correlation between FRA3B expression and cigarette smoking. Gene Chromosomes Canc 2002; 34:333-40; PMID:12007194; http://dx.doi.org/10.1002/gcc.10061
14. Hanahan D, Weinberg RA. The hallmarks of cancer. Cell 2000; 100:57-70; PMID:10647931; http://dx.doi.org/10.1016/S0092-8674(00)81683-9
15. D'Agostini F. Early Loss of Fhit in the Respiratory Tract of Rodents Exposed to Environmental Cigarette Smoke. Cancer Res 2006; 66:3936-41; PMID:16585223; http://dx.doi.org/10.1158/0008-5472.CAN-05-3666
16. Kim JS. Aberrant methylation of the FHIT gene in chronic smokers with early stage squamous cell carcinoma of the lung. Carcinogenesis 2004; 25:2165-71; PMID:15231689; http://dx.doi.org/10.1093/carcin/bgh217
17. Sozzi G, Sard L, De Gregorio L, Marchetti A, Musso K, Buttitta F, Tornielli S, Pellegrini S, Veronese ML, Manenti G, et al. Association between cigarette smoking and FHIT gene alterations in lung cancer. Cancer Res 1997; 57:2121-3; PMID:9187107
18. Sozzi G, Pastorino U, Moiraghi L, Tagliabue E, Pezzella F, Ghirelli C, Tornielli S, Sard L, Huebner K, Pierotti MA. Loss of FHIT function in lung cancer and preinvasive bronchial lesions. Cancer Res 1998; 58:5032-7; PMID:9823304
19. Ferrandiz ML, Devesa I. Inducers of heme oxygenase-1. Curr pharm design 2008; 14:473-86; PMID: 18289074; http://dx.doi.org/10.2174/138161208783597399
20. Gozzelino R, Jeney V, Soares MP. Mechanisms of Cell Protection by Heme Oxygenase-1. Annu Rev Pharmacol Toxicol 2010; 50:323-54; PMID: 20055707; http://dx.doi.org/10.1146/annurev.pharmtox.010909.105600
21. Joannes A, Grelet S, Duca L, Gilles C, Kileztky C, Dalstein V, Birembaut P, Polette M, Nawrocki-Raby B. Fhit Regulates EMT Targets through an EGFR/Src/ERK/Slug Signaling Axis in Human Bronchial Cells. Mol Cancer Res 2014; 12(5):775-83; PMID:24464917; http://dx.doi.org/10.1158/1541-7786.MCR-13-0386-T
22. Joannes A, Bonnomet A, Bindels S, Polette M, Gilles C, Burlet H, Cutrona J, Zahm J-M, Birembaut P, Nawrocki-Raby B. Fhit regulates invasion of lung tumor cells. Oncogene 2009; 29:1203-13; PMID: 19935706; http://dx.doi.org/10.1038/onc.2009.418
23. Saldivar JC, Miuma S, Bene J, Hosseini SA, Shibata H, Sun J, Wheeler LJ, Mathews CK, Huebner K. Initiation of Genome Instability and Preneoplastic Processes through Loss of Fhit Expression. PLoS Genet 2012; 8:e1003077; PMID:23209436; http://dx.doi.org/10.1371/journal.pgen.1003077
24. Saldivar JC, Bene J, Hosseini SA, Miuma S, Horton S, Heerema NA, Huebner K. Characterization of the role of Fhit in suppression of DNA damage. AdvBiol Regulation 2013; 53:77-85; PMID:23102829; http://dx.doi.org/10.1016/j.jbior.2012.10.003
25. Miuma S, Saldivar JC, Karras JR, Waters CE, Paisie CA, Wang Y, Jin V, Sun J, Druck T, Zhang J, et al. Fhit deficiency-induced global genome instability promotes mutation and clonal expansion. PLoS ONE 2013; 8:e80730-0; PMID:24244712; http://dx.doi.org/10.1371/journal.pone.0080730
26. Trapasso F, Pichiorri F, Gaspari M, Palumbo T, Aqeilan RI, Gaudio E, Okumura H, Iuliano R, Di Leva G, Fabbri M. Fhit interaction with ferredoxin reductase triggers generation of reactive oxygen species and apoptosis of cancer cells. J Biol Chem 2008; 283:13736-44; PMID:18319262; http://dx.doi.org/10.1074/jbc.M709062200
27. Pichiorri F, Okumura H, Nakamura T, Garrison PN, Gasparini P, Suh S-S, Druck T, McCorkell KA, Barnes LD, Croce CM. Correlation of fragile histidine triad (Fhit) protein structural features with effector interactions and biological functions. J Biol Chem 2009; 284:1040-9; PMID:19004824; http://dx.doi.org/10.1074/jbc.M806638200
28. Hori R. Gene Transfection of H25A Mutant Heme Oxygenase-1 Protects Cells against Hydroperoxide-induced Cytotoxicity. J Biol Chem 2002; 277:10712-8; PMID:11786534; http://dx.doi.org/10.1074/jbc.M107749200
29. Clark JE, Green CJ, Motterlini R. Involvement of the heme oxygenase-carbon monoxide pathway in keratinocyte proliferation. Biochem Bioph Res Co 1997; 241:215-20; PMID:9425252; http://dx.doi.org/10.1006/bbrc.1997.7742
30. Seldon MP, Silva G, Pejanovic N, Larsen R, Gregoire IP, Filipe J, Anrather J, Soares MP. Heme oxygenase-1 inhibits the expression of adhesion molecules associated with endothelial cell activation via inhibition of NF-kappaB RelA phosphorylation at serine 276. J Immunol 2007; 179:7840-51; PMID:18025230; http://dx.doi.org/10.4049/jimmunol.179.11.7840
31. Jozkowicz A, Huk I, Nigisch A, Weigel G, Dietrich W, Motterlini R, Dulak J. Heme oxygenase and angiogenic activity of endothelial cells: stimulation by carbon monoxide and inhibition by tin protoporphyrin-IX. Antioxid Redox Signal 2003; 5:155-62; PMID:12716475; http://dx.doi.org/10.1089/152308603764816514
32. Nowis D, Legat M, Grzela T, Niderla J, Wilczek E, Wilczynski GM, Głodkowska E, Mrówka P, Issat T, Dulak J, et al. Heme oxygenase-1 protects tumor cells against photodynamic therapy-mediated cytotoxicity. Oncogene 2006; 25:3365-74; PMID: 16462769; http://dx.doi.org/10.1038/sj.onc.1209378
33. Jozkowicz A, Was H, Dulak J. Heme Oxygenase-1 in Tumors: Is It a False Friend? Antioxid Redox Signal 2007; 9:2099-118; PMID:17822372; http://dx.doi.org/10.1089/ars.2007.1659
34. Nyunoya T, Monick MM, Klingelhutz A, Yarovinsky TO, Cagley JR, Hunninghake GW. Cigarette Smoke Induces Cellular Senescence. Am J Resp Cell Mol Biol 2006; 35:681-8; PMID:16840774; http://dx.doi.org/10.1165/rcmb.2006-0169OC
35. Ramirez RD, Sheridan S, Girard L, Sato M, Kim Y, Pollack J, Peyton M, Zou Y, Kurie JM, Dimaio JM, et al. Immortalization of human bronchial epithelial

cells in the absence of viral oncoproteins. Cancer Res 2004; 64:9027-34; PMID:15604268; http://dx.doi.org/10.1158/0008-5472.CAN-04-3703
36. Sato M. Multiple Oncogenic Changes (K-RASV12, p53 Knockdown, Mutant EGFRs, p16 Bypass, Telomerase) Are Not Sufficient to Confer a Full Malignant Phenotype on Human Bronchial Epithelial Cells. Cancer Res 2006; 66:2116-28; PMID:16489012; http://dx.doi.org/10.1158/0008-5472.CAN-05-2521
37. Holschneider CH. The Fragile Histidine Triad Gene: A Molecular Link Between Cigarette Smoking and Cervical Cancer. Clin Cancer Res 2005; 11:5756-63; PMID:16115913; http://dx.doi.org/10.1158/1078-0432.CCR-05-0234
38. Tseng JE, Kemp BL, Khuri FR, Kurie JM, Lee JS, Zhou X, Liu D, Hong WK, Mao L. Loss of Fhit is frequent in stage I non-small cell lung cancer and in the lungs of chronic smokers. Cancer Res 1999; 59:4798-803; PMID:10519387
39. Choi AM, Alam J. Heme oxygenase-1: function, regulation, and implication of a novel stress-inducible protein in oxidant-induced lung injury. Am J Resp Cell Mol Biol 1996; 15:9-19; PMID:8679227; http://dx.doi.org/10.1165/ajrcmb.15.1.8679227
40. Maines MD, Gibbs PEM. 30 some years of heme oxygenase: From a "molecular wrecking ball" to a 'mesmerizing' trigger of cellular events. Biochem Bioph Res Commun 2005; 338:568-77; PMID:16183036; http://dx.doi.org/10.1016/j.bbrc.2005.08.121
41. Klingelhutz AJ, Qian Q, Phillips SL, Gourronc FA, Darbro BW, Patil SR. Amplification of the chromosome 20q region is associated with expression of HPV-16 E7 in human airway and anogenital epithelial cells. Virology 2005; 340:237-44; PMID: 16051300; http://dx.doi.org/10.1016/j.virol.2005.06.027
42. Kiyono T, Foster SA, Koop JI, McDougall JK, Galloway DA, Klingelhutz AJ. Both Rb/p16INK4a inactivation and telomerase activity are required to immortalize human epithelial cells. Nature 1998; 396:84-8; PMID:9817205; http://dx.doi.org/10.1038/23962
43. Rimessi A, Marchi S, Fotino C, Romagnoli A, Huebner K, Croce CM, Pinton P, Rizzuto R. Intramitochondrial calcium regulation by the FHIT gene product sensitizes to apoptosis. Proc Nat Acad Sci 2009; 106:12753-8; MPID:19622739; http://dx.doi.org/10.1073/pnas.0906484106
44. Nakagawa Y, Akao Y. Fhit protein inhibits cell growth by attenuating the signaling mediated by nuclear factor-κB in colon cancer cell lines. Exp Cell Res 2006; 312:2433-42; PMID:16733051; http://dx.doi.org/10.1016/j.yexcr.2006.04.004
45. Mir Mohammadrezaei F, Mohseni kouchesfehani H, Montazeri H, Gharghabi M, Ostad SN, Ghahremani MH. Signaling crosstalk of FHIT, CHK2 and p38 in etoposide induced growth inhibition in MCF-7 cells. Cell Signal 2013; 25:126-32; PMID:23000346; http://dx.doi.org/10.1016/j.cellsig.2012.09.019
46. Lau WKW, Chan SCH, Law ACK, Ip MSM, Mak JCW. The role of MAPK and Nrf2 pathways in ketanserin-elicited attenuation of cigarette smoke-induced IL-8 production in human bronchial epithelial cells. Toxicol Sci 2012; 125:569-77; PMID: 22048642; http://dx.doi.org/10.1093/toxsci/kfr305
47. Maunders H, Patwardhan S, Phillips J, Clack A, Richter A. Human bronchial epithelial cell transcriptome: gene expression changes following acute exposure to whole cigarette smoke in vitro. AJP: Lung Cell Mol Phys 2007; 292:L1248-56; PMID: 22048642; http://dx.doi.org/10.1152/ajplung.00290.2006
48. Pickett G, Seagrave J, Boggs S, Polzin G, Richter P, Tesfaigzi Y. Effects of 10 cigarette smoke condensates on primary human airway epithelial cells by comparative gene and cytokine expression studies. Toxicol Sci 2010; 114:79-89; PMID:20015843; http://dx.doi.org/10.1093/toxsci/kfp298
49. Gümüş ZH, Du B, Kacker A, Boyle JO, Bocker JM, Mukherjee P, Subbaramaiah K, Dannenberg AJ, Weinstein H. Effects of tobacco smoke on gene expression and cellular pathways in a cellular model of oral leukoplakia. Cancer Prevention Res 2008; 1:100-11; PMID:19138943; http://dx.doi.org/10.1158/1940-6207.CAPR-08-0007
50. Baglole CJ, Maggirwar SB, Gasiewicz TA, Thatcher TH, Phipps RP, Sime PJ. The aryl hydrocarbon receptor attenuates tobacco smoke-induced cyclooxygenase-2 and prostaglandin production in lung fibroblasts through regulation of the NF-kappaB family member RelB. J Biol Chem 2008; 283:28944-57; PMID:18697742; http://dx.doi.org/10.1074/jbc.M800685200
51. Jorquera G, Juretic N, Jaimovich E, Riveros N. Membrane depolarization induces calcium-dependent upregulation of Hsp70 and Hmox-1 in skeletal muscle cells. AJP: Cell Phys 2009; 297:C581-90.
52. Alam J, Cook JL. How Many Transcription Factors Does It Take to Turn On the Heme Oxygenase-1 Gene? Am J Resp Cell Mol Biol 2006; 36:166-74; PMID:16990612; http://dx.doi.org/10.1165/rcmb.2006-0340TR
53. Zhang X, Bedard EL, Potter R, Zhong R, Alam J, Choi AMK, Lee PJ. Mitogen-activated protein kinases regulate HO-1 gene transcription after ischemia-reperfusion lung injury. Am J Physiol Lung Cell Mol Physiol 2002; 283:L815-29; PMID:12225959; http://dx.doi.org/10.1152/ajplung.00485.2001
54. Sun J, Hoshino H, Takaku K, Nakajima O, Muto A, Suzuki H, Tashiro S, Takahashi S, Shibahara S, Alam J, et al. Hemoprotein Bach1 regulates enhancer availability of heme oxygenase-1 gene. EMBO J 2002; 21:5216-24; PMID:12356737; http://dx.doi.org/10.1093/emboj/cdf516
55. Reichard JF, Motz GT, Puga A. Heme oxygenase-1 induction by NRF2 requires inactivation of the transcriptional repressor BACH1. Nucleic Acids Res 2007; 35:7074-86; PMID:17942419; http://dx.doi.org/10.1093/nar/gkm638
56. Loboda A, Was H, Jozkowicz A, Dulak J. Janus face of Nrf2-HO-1 axis in cancer–friend in chemoprevention, foe in anticancer therapy. Lung Cancer (Amsterdam, Netherlands) 2008; 60:1; PMID:18063196; http://dx.doi.org/10.1016/j.lungcan.2007.10.024
57. Zenke-Kawasaki Y, Dohi Y, Katoh Y, Ikura T, Ikura M, Asahara T, Tokunaga F, Iwai K, Igarashi K. Heme Induces Ubiquitination and Degradation of the Transcription Factor Bach1. Mol Cell Biol 2007; 27:6962-71; PMID:17682061; http://dx.doi.org/10.1128/MCB.02415-06
58. Draganescu A, Hodawadekar SC, Gee KR, Brenner C. Fhit-nucleotide specificity probed with novel fluorescent and fluorogenic substrates. J Biol Chem 2000; 275:4555-60; PMID:10671479; http://dx.doi.org/10.1074/jbc.275.7.4555
59. Brenner C, Pace HC, Garrison PN, Robinson AK, Rosler A, Liu XH, Blackburn GM, Croce CM, Huebner K, Barnes LD. Purification and crystallization of complexes modeling the active state of the fragile histidine triad protein. Protein Eng 1997; 10:1461-3; PMID:9543008; http://dx.doi.org/10.1093/protein/10.12.1461
60. Pace HC, Garrison PN, Robinson AK, Barnes LD, Draganescu A, Rosler A, Blackburn GM, Siprashvili Z, Croce CM, Huebner K, et al. Genetic, biochemical, and crystallographic characterization of Fhit-substrate complexes as the active signaling form of Fhit. Proc Natl Acad Sci USA 1998; 95:5484-9; PMID: 9576908; http://dx.doi.org/10.1073/pnas95.10.5484
61. Campiglio M, Bianchi F, Andriani F, Sozzi G, Tagliabue E, Ménard S, Roz L. Diadenosines as FHIT-ness instructors. J Cell Physiol 2006; 208:274-81; PMID:16547961; http://dx.doi.org/10.1002/jcp.20633
62. Fisher DI, McLennan AG. Correlation of intracellular diadenosine triphosphate (Ap3A) with apoptosis in Fhit-positive HEK293 cells. Cancer Lett 2008; 259:186-91; PMID:18006149; http://dx.doi.org/10.1016/j.canlet.2007.10.007
63. Jovanovic A, Alekseev AE, Terzic A. Intracellular diadenosine polyphosphates: a novel family of inhibitory ligands of the ATP-sensitive K+ channel. Biochem Pharmacol 1997; 54:219-25; PMID:9271325; http://dx.doi.org/10.1016/S0006-2952(97)00262-1
64. Brevet A, Plateau P, Best-Belpomme M, Blanquet S. Variation of Ap4A and other dinucleoside polyphosphates in stressed Drosophila cells. J Biol Chem 1985; 260:15566-70; PMID:4066685
65. Bochner BR, Lee PC, Wilson SW, Cutler CW, Ames BN. AppppA and related adenylylated nucleotides are synthesized as a consequence of oxidation stress. Cell 1984; 37:225-32; PMID:6373012; http://dx.doi.org/10.1016/0092-8674(84)90318-0
66. Brenner C, Bieganowski P, Pace HC, Huebner K. The histidine triad superfamily of nucleotide-binding proteins. J Cell Physiol 1999; 181:179-87; PMID:10497298; http://dx.doi.org/10.1002/(SICI)1097-4652(199911)181:2%3c179::AID-JCP1%3e3.0.CO;2-8
67. Brenner C. Hint, Fhit, and GalT: function, structure, evolution, and mechanism of three branches of the histidine triad superfamily of nucleotide hydrolases and transferases. Biochemistry 2002; 41:9003-14; PMID:12119013; http://dx.doi.org/10.1021/bi025942q
68. McLennan AG, Barnes LD, Blackburn GM, Brenner C, Guranowski A, Miller AD, Rovira JM, Rotllán P, Soria B, Tanner JA. Recent progress in the study of the intracellular functions of diadenosine polyphosphates. Drug develop res 2001; 52:249-59; http://dx.doi.org/10.1002/ddr.1122
69. Ishii H, Mimori K, Ishikawa K, Okumura H, Pichiorri F, Druck T, Inoue H, Vecchione A, Saito T, Mori M, et al. Fhit-Deficient Hematopoietic Stem Cells Survive Hydroquinone Exposure Carrying Precancerous Changes. Cancer Res 2008; 68:3662-70; PMID:18483248; http://dx.doi.org/10.1158/0008-5472.CAN-07-5687
70. Ottey M, Han S-Y, Druck T, Barnoski BL, McCorkell KA, Croce CM, Raventos-Suarez C, Fairchild CR, Wang Y, Huebner K. Fhit-deficient normal and cancer cells are mitomycin C and UVC resistant. Br J Cancer 2004; 91(9):1669-77; PMID:15494723; http://dx.doi.org/10.1038/sj.bjc.6602058
71. Andriani F, Perego P, Carenini N, Sozzi G, Roz L. Increased Sensitivity to Cisplatin in Non–Small Cell Lung Cancer Cell Lines after FHIT Gene Transfer. NEO 2006; 8:9-17; PMID:16533421; http://dx.doi.org/10.1593/neo.05517
72. Tomasz M, Lipman R, Chowdary D, Pawlak J, Verdine GL, Nakanishi K. Isolation and structure of a covalent cross-link adduct between mitomycin C and DNA. Science 1987; 235:1204-8; PMID:3103215; http://dx.doi.org/10.1126/science.3103215
73. Pommier Y. Eukaryotic DNA topoisomerase I: genome gatekeeper and its intruders, camptothecins. Semin oncol 1996; 23(1 Suppl 3):3-10; PMID: 8633251
74. Siddik ZH. Cisplatin: mode of cytotoxic action and molecular basis of resistance. Oncogene 2003; 22:7265-79; PMID:14576837; http://dx.doi.org/10.1038/sj.onc.1206933
75. Berndtsson M, Hägg M, Panaretakis T, Havelka AM, Shoshan MC, Linder S. Acute apoptosis by cisplatin requires induction of reactive oxygen species but is not associated with damage to nuclear DNA. Int J Cancer 2006; 120:175-80; PMID:17044026; http://dx.doi.org/10.1002/ijc.22132
76. Park JY, Seo YR. Enhancement of mitomycin C-induced apoptosis in Nrf2-deficient human colon cancer cells. Mol Cell Toxicol 2010; 6:51-6; http://dx.doi.org/10.1007/s13273-010-0007-4

77. Wang Y, Gray JP, Mishin V, Heck DE, Laskin DL, Laskin JD. Distinct Roles of Cytochrome P450 Reductase in Mitomycin c Redox Cycling and Cytotoxicity. Mol Cancer Therap 2010; 9:1852-63; PMID:20501808; http://dx.doi.org/10.1158/1535-7163.MCT-09-1098

78. Komiyama T, Kikuchi T, Sugiura Y. Generation of hydroxyl radical by anticancer quinone drugs, carbazilquinone, mitomycin C, aclacinomycin A and adriamycin, in the presence of NADPH-cytochrome P-450 reductase. Biochem Pharmacol 1982; 31:3651-6; PMID:6295407; http://dx.doi.org/10.1016/0006-2952(82)90590-1

79. Li Y, Rory Goodwin C, Sang Y, Rosen EM, Laterra J, Xia S. Camptothecin and Fas receptor agonists synergistically induce medulloblastoma cell death: ROS-dependent mechanisms. Anticancer Drugs 2009; 20:770-8; PMID:19633536; http://dx.doi.org/10.1097/CAD.0b013e32832fe472